

Original paper

# Amphibole and pyroxene as indicators of alkaline conditions in banded carbonatite-like marbles from Bližná, Český Krumlov Unit, Moldanubian Zone

Pavína RADKOVÁ<sup>1,2\*</sup>, Milan NOVÁK<sup>1</sup>, Jan CEMPIREK<sup>1</sup>, Stanislav HOUZAR<sup>3</sup>, Radek ŠKODA<sup>1</sup>

<sup>1</sup> Department of Geological Sciences, Faculty of Science, Masaryk University, Kotlářská 2, CZ-611 37 Brno, Czech Republic; radkova4@uniba.sk

<sup>2</sup> Department of Mineralogy, Petrography and Geology of Mineral Deposits, Faculty of Natural Sciences, Comenius University, Ilkovičova 6, 842 15 Bratislava, Slovakia

<sup>3</sup> Department of Mineralogy and Petrography, Moravian Museum, Zelný trh 6, 659 37 Brno, Czech Republic

\* Corresponding author



Amphiboles and diopside occur in several distinct mineral assemblages in banded carbonatite-like marbles from the Bližná graphite mine, Český Krumlov Unit, Moldanubian Zone. The carbonatite-like marble is interlayered with dominant ordinary metacarbonates as a single continuous stratabound layer, up to 3–4 m thick. It is enriched in elements typical for carbonatites (REE, Y, Th, Sr, Nb, Zr, and Mo) and contains accessory betafite-pyrochlore and uranorthorite along with molybdenite, sulfides (e.g., pyrite, pyrrhotite) and oxides (e.g., magnetite, ilmenite). Detailed study of thin sections in optical microscope and BSE images as well as results of EMPA revealed three distinct mineral assemblages – richterite + forsterite (RF) assemblage ( $Rht + Fo + Cal > Dol > Phl + Di$ ), Na-rich actinolite + diopside (AD) assemblage ( $Di + Act + Rht + Cal > Phl$ ) and magnesio-hastingsite + diopside (HD) assemblage ( $Mhst + Di + Cal > Ab + Phl$ ). The distinct amphibole species found within the individual assemblages exhibit complex textural relations and crystallized in several prograde and retrograde stages. The following amphibole species were recognized in the individual assemblages: RF – (richterite > ferri-winchite > tremolite, edenite), AD – (actinolite > ferri-winchite; richterite > ferri-katophorite; magnesio-riebeckite), HD – (magnesio-hastingsite; ferri-winchite, actinolite). They differ especially in  $Mg/(Mg + Fe_{tot})$  ratio and concentrations of F. Diopside contains up to 17 mol. % of the aegirine component and albite is Fe, Ba-enriched ( $\leq 0.69$  wt. % BaO and  $\leq 0.50$  wt. %  $Fe_2O_{3tot}$ ). The composition of amphiboles and pyroxenes indicates the alkaline environment of their formation; unusually high  $Fe_2O_3$  contents in albite plagioclase have known counterparts in alkaline pegmatites and some carbonatite dykes. The following options of potential origin of the carbonatite-like marble from Bližná are discussed: (i) metacarbonates potentially with Na- and Na,Ca-carbonates and sulfate admixture; (ii) admixture of alkaline volcanodetrific component during carbonate sedimentation; (iii) metamorphosed carbonatites enclosed in ordinary sedimentary metacarbonate; (iv) Na-rich metasomatites characterized by mineral assemblages with Na,Fe,F-enriched amphiboles, diopside with high aegirine component and albite. With regard to the observed mineral assemblages, textures and composition of minerals, we can exclude (i) marine evaporates, whereas the other options (ii), (iii) and (iv) are, in general, possible. The amphiboles observed in the Bližná carbonatite-like marble are unique within the Bohemian Massif and distinctly different from amphiboles found in metacarbonates with evaporite component.

**Keywords:** alkali amphibole, pyroxene, carbonatite-like marble, Český Krumlov unit, Moldanubian Zone, Bohemian Massif

**Received:** 16 August 2021; **accepted:** 8 December 2021; **handling editor:** J. Kotková

## 1. Introduction

Amphiboles are typical accessory to major rock-forming minerals in metacarbonates from supracrustal complexes metamorphosed from greenschist to granulite facies. Calcic amphiboles (tremolite, actinolite, magnesio-hornblende, edenite, pargasite, magnesio-hastingsite) are dominant in metacarbonates of sedimentary origin (e.g., Deer et al. 1997), whereas sodic-calcic amphiboles (richterite, winchite) and sodic amphiboles (magnesio-riebeckite, riebeckite, arfvedsonite) occur along with aegirine-rich clinopyroxene in specific carbonate lithologies including a variety of carbonatites *s.l.* (e.g., Mitchell 2005; Martin

2007). Alkali-rich amphiboles and pyroxenes from carbonatites *s.s.* were studied in detail in numerous papers (e.g., Reguir et al. 2012 and references therein; Chudy 2013) whereas amphiboles and pyroxenes from metacarbonates enclosed in evident sedimentary lithologies with geochemical signature distinct from ordinary marbles have been examined only sporadically (e.g., Houzar 2004; Houzar et al. 2017), or for special purposes such as research of marble-hosted gem deposits (e.g., Dzikowski et al. 2014; Garnier et al. 2005, 2008; Feneyrol et al. 2012).

Banded carbonatite-like marble interlayered with dominant ordinary metacarbonates from Bližná, Český Krumlov Varied Unit, Moldanubian Zone, is enriched in elements

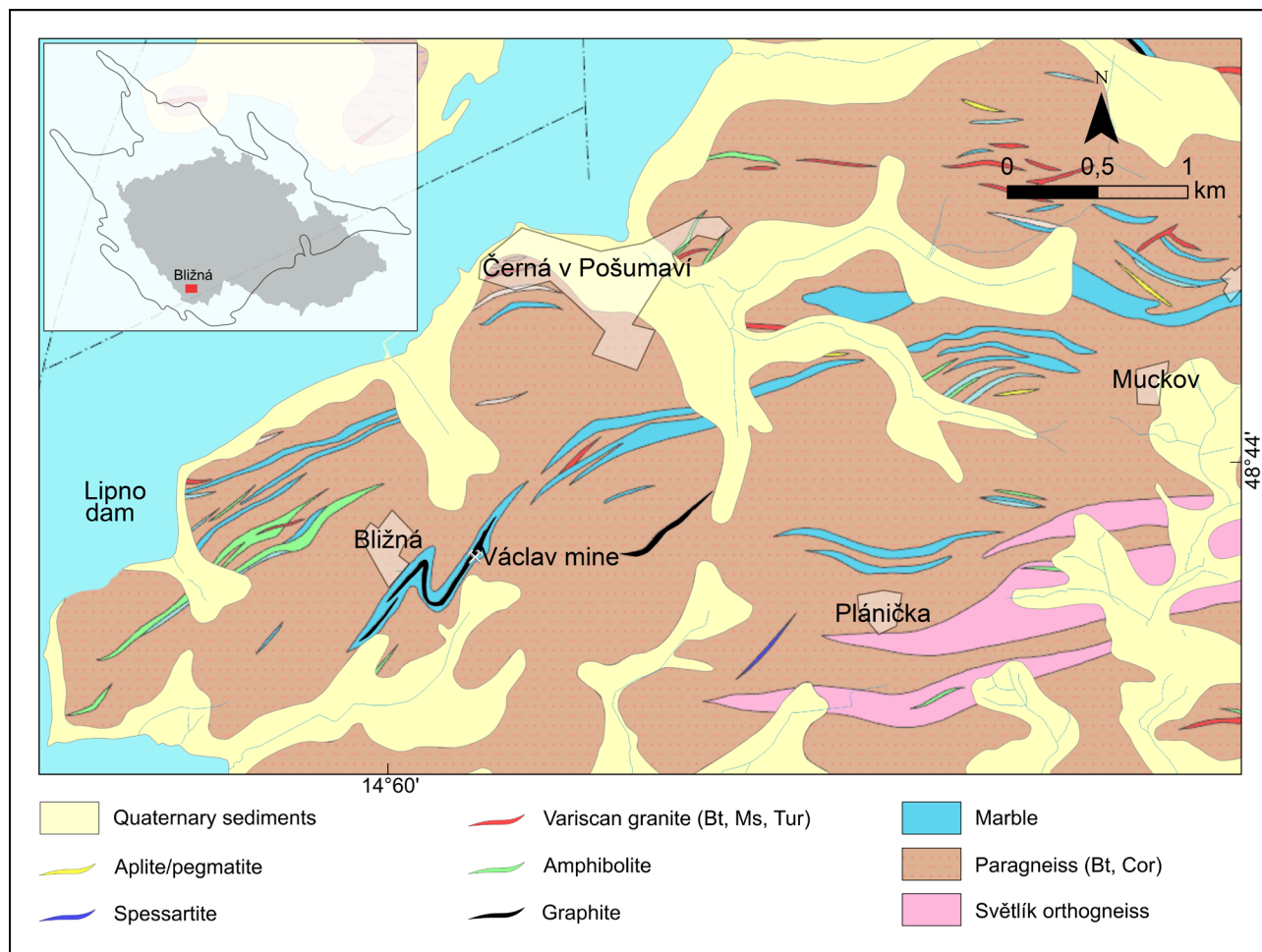


Fig. 1 Schematic geological map of the Bližná surroundings, Český Krumlov Unit. Modified from Vrána et al. (2010).

typical for carbonatites (REE, Y, Th, Sr, Nb, Zr, and Mo) and contains accessory betafite-pyroxene, uranothorite and molybdenite along with other accessory minerals (Šarbach et al. 1985; Veselovský et al. 1987; Drábek et al. 1999; Drábek and Stein 2015; Novák et al. 2012; Radková 2017). We examined textural relations, mineral assemblages and chemical composition of abundant amphibole and minor pyroxene and olivine from this unique carbonatite-like marble to reveal their compositional variability and geochemical signature in relation to ordinary carbonatites (Reguir et al. 2012 and references therein). A possible origin of the carbonatite-like marble protolith is discussed.

## 2. Geological setting

### 2.1. Lithology of the Český Krumlov Varied Unit

This area is built by medium- to high-grade plagioclase–biotite paragneisses with common intercalations of metacarbonates (marbles to silicate-rich and graphite-

bearing marbles), quartzitic and graphite paragneisses, calc–silicate rocks and locally of amphibolites and amphibole gneisses (Fig. 1). A sedimentary origin of marbles in an oxidic shallow marine environment is significantly prevalent and well documented (Čížek et al. 1984; Suk 1974). The rocks belong to the metasedimentary complex of the Drosendorf Unit (e.g., Zoubek et al. 1988; Jenček and Vajner 1968; Högelsberger 1989; Cháb et al. 2008; Vrána et al. 2010; Houzar et al. 2017). Organic matter and hydrogen sulfide accumulated in local anoxic conditions from lagoons were transformed to graphite layers (Hladíková et al. 1993; Schrauder et al. 1993). The Paleozoic age of the Drosendorf Unit is frequently presumed; however, an early Neoproterozoic protolith age of 800–900 Ma was inferred for the analogous marbles of the Drosendorf Unit in Austria, based on their low  $^{87}\text{Sr}/^{86}\text{Sr}$  ratios (Frank et al. 1990, 1992).

### 2.2. Metacarbonates from Bližná

In the abandoned Václav graphite mine near Bližná, Drábek et al. (1999) distinguished three distinct types of



**Fig. 2** Banded carbonatite-like marble, the third level of the Václav graphite mine. The dark layers are silicate-rich; note detailed folding of the rock.

metacarbonates based on their geochemistry, bulk mineral assemblages, and the isotopic composition of Sr, C and O: (i) Ordinary marble (OM) similar to other marbles within the Český Krumlov Varied Unit, (ii) carbonatite-like marble (CLM), and (iii) transitional marble (TM). The latter two occur as a single continuous stratabound layer, up to 3–4 m thick, only in the close footwall of the graphite horizon on the 3<sup>rd</sup> level of the mine across the air pit K10 (Fig. 2).

The abundant (i) *ordinary calcite to calcite-dolomite marbles* (OM), locally banded, with common silicates (tremolite, phlogopite, diopside, forsterite, chlorite) and pyrite, pyrrhotite, and graphite, form large nodular bodies up to 30 m thick (Vrána et al. 2010). Based on their textural, mineralogical and geochemical characteristics, they were interpreted as metacarbonates from a shallow marine environment (Houzar et al. 2017).

Rare (ii) *carbonatite-like calcite marbles* (CLM) are texturally heterogeneous and commonly rich in silicates (amphiboles, phlogopite, diopside, forsterite, antigorite, talc; Drábek et al. 1999). They are characterized by highly heterogeneous chemical composition with variable but locally very high concentrations of Mo, Nb, Zr, Th and REE (Drábek et al. 1999, 2017; Drábek and Stein 2015; Novák et al. 2012). Sulfide-rich portions with pyrrhotite, pyrite, molybdenite, chalcopyrite, galenite, and sphalerite are somewhat randomly distributed. In contrast, locally common accessory REE-minerals (Th, REE-rich betafite, uranothorite), fluorapatite, ilmenite with rare columbite inclusions, and zircon are concentrated in a single layer (Radková 2017). Molybdenite dated using Re–Os method at ~495 Ma records regional amphibolite-facies metamorphism (Drábek and Stein 2003).

Rare (iii) calcite to calcite-dolomite marbles with transitional composition between CLM and OM (*transitional marble*; TM) have mineralogy similar to (ii) except that

they contain moderate to low concentrations of Mo, Nb, Zr and REE only (Drábek et al. 1999). Abundant calcite to calcite-dolomite marbles (OM) from the Český Krumlov Unit, including locality Bližná with tremolite, forsterite and diopside have been interpreted as metacarbonates from a shallow-marine lagoonal environment, locally with evaporite admixture due to the presence of Cl-rich scapolite (Kadounová 1987; Kříbek 1988; Kříbek et al. 1997), whereas CLM and TM were suggested to contain variable quantities of volcanodetritic materials derived from alkaline volcanism (Drábek et al. 1999, 2017). However, alkaline metabasites or other alkaline rocks have not been found in the Černá region. Moreover, metacarbonate bodies with carbonatite-like geochemical signature are known from Muckov, the Český Krumlov Unit (Fig. 1), where a single marble sample yielded elevated contents of Zr, Nb, U, Th and REE (Houzar and Novák 2002).

### 3. Methodology

#### 3.1. Samples

Amphiboles and associated minerals were studied in thin sections obtained from a large fragment of banded metacarbonate collected in the Václav graphite mine, Bližná. The fragment consists of carbonatite-like marble (CLM) and transitional marble (TM) using the terms proposed by Drábek et al. (1999). Seven thin sections were prepared from the fragment (Fig. 3).

#### 3.2. Chemical composition

Minerals of distinct bands in metacarbonate were analyzed with a Cameca SX100 electron microprobe in wavelength-dispersive mode at the Joint Laboratory of Electron Microscopy and Microanalysis of the Department of Geological Sciences, Masaryk University, Brno, Czech Republic. Silicates and carbonates were analyzed at accelerating voltage of 15 kV, beam current of 10 nA, and beam diameter 5  $\mu\text{m}$ , using following standards: Na (albite); K, Al, Si (sanidine); Ca (wollastonite); Sr (synthetic  $\text{SrSO}_4$ ); Ba (synthetic  $\text{BaSO}_4$ ); Ti (titanite); Mg (forsterite); Mn (spessartine); Fe (almandine); Zn (gahnite); Ni (synthetic  $\text{Ni}_2\text{SiO}_4$ ); Cr (chromite); F (topaz); Cl (vanadinite); Sc and V (synthetic  $\text{ScVO}_4$ ). Major elements were measured 10 to 20 s and the minor and trace elements 40 and 60 s, respectively, on the peak and a half of the peak time for background counts on high- and low-energy sides of the peak. Raw data were converted into concentrations using appropriate *X-PHI* matrix corrections (Merlet 1994). All abbreviations of mineral names are according to Warr (2021).

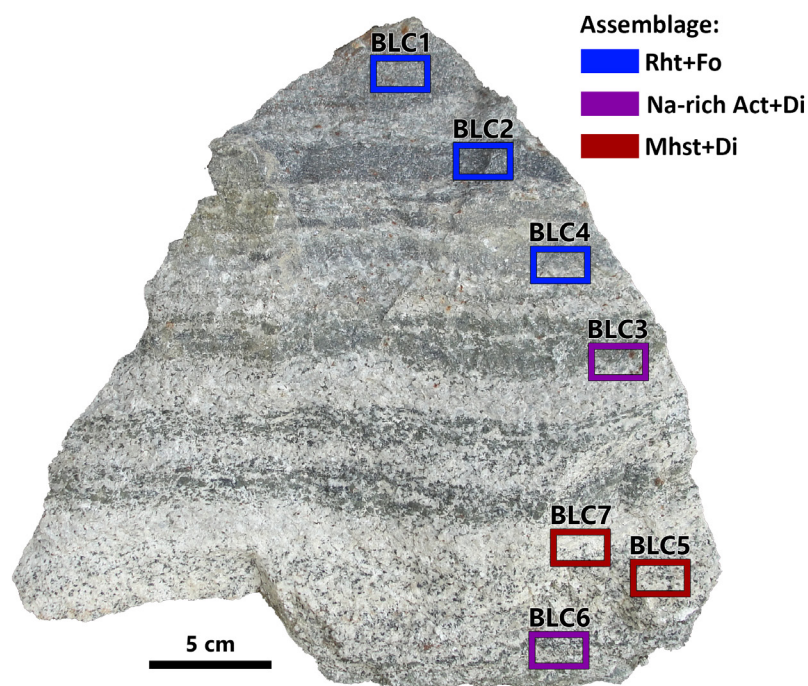


Fig. 3 Large fragment of banded meta-carbonate; the position of the individual thin sections is marked.

Tab. 1 Mineral assemblages and amphibole proportions of individual samples. a – major phases of mineral assemblages.

assemblage & sample		primary minerals										secondary minerals				
		Cal	Dol	Fo	Di	Phl	Rht	Act	Ba-Phl	Mhst	Ab	Mrbk	Fwnc	Tlc	Srp	Chl
RF	BLC 1	A	C	A	R	R	A								C <sup>Fo</sup>	R <sup>Phl</sup>
	BLC 2	A	C	A			A								C <sup>Fo</sup>	
	BLC 4	A	R	C		C	A								A <sup>Fo, Rht</sup>	
AD	BLC 3	A			C		A	A				C		R <sup>Act</sup>	C <sup>Di, Rht</sup>	
	BLC 6	A			A	R	C	A								R <sup>Phl</sup>
HD	BLC 5	A			A				R	A	R		C <sup>Mhst</sup>		R <sup>Di</sup>	
	BLC 7	A			C				R	A	C		C <sup>Mhst</sup>		R <sup>Di</sup>	

A = abundant, C = common, R = rare; upper index mineral abbreviations with secondary minerals indicate the replaced primary phase.

Tab. 1b – proportions of the amphibole species.

assemblage & sample		richterite	actinolite	magnesio-hastingsite	magnesio-riebeckite	ferri-winchite
RF	BLC 1	Rht ~ Ed				
	BLC 2	Rht > Tr > Fwnc, Ed				
	BLC 4	Rht >> Fwnc				
AD	BLC 3	Rht	Act > Fwnc		Mrbk	
	BLC 6	Rht	Act > Fwnc			
HD	BLC 5			Mhst >> Fktp		Fwnc >> Act
	BLC 7			Mhst >> Fktp		Fwnc >> Act

## 4. Results

The individual bands differ in grain size, textures and mainly in mineral contents (Tab. 1a) and the chemical

composition of rock-forming minerals (amphiboles, pyroxene, olivine and phlogopite). Several amphibole species (Leake et al. 1997, Hawthorne et al. 2012) were identified (Tab. 1b); more details about the chemical

compositions are given in section 4.2. Detailed study of thin sections using an optical microscope and BSE images, as well as results of EMPA, revealed three distinct mineral assemblages named according to the dominant primary mineral assemblage – richterite + forsterite assemblage (RF), Na-rich actinolite + diopside assemblage (AD) and magnesio-hastingsite + diopside assemblage (HD). Due to the heterogeneous compositions of amphiboles, we used the name of the dominant amphibole species in the descriptions of the defined mineral assemblages (Tab. 1a,b).

#### 4.1. Mineral assemblages of the banded carbonatite-like marble

**The richterite + forsterite assemblage** (samples BLC 1, BLC 2, and BLC 4; Fig. 3) occurs in fine- (~0.5 mm) to medium-grained (~2 mm) marble bands. Their characteristic overall mineral assemblage is  $Rht + Fo + Cal > Dol > Phl + Di$ . The rock shows parallel layers of  $Fo + Cal + Dol$  and  $Rht + Cal + Dol$ , both usually ~5–10 mm thick, in a

carbonate-dominated matrix (see also Tab. 1). The occurrence of minor dolomite and common forsterite is distinct from the other assemblages (Tab. 1). Dolomite mainly occurs as subhedral grains, often adjacent to silicates (Fig. 4a,b), or in fine-grained symplectite together with calcite (Fig. 4b). Microscopic symplectites of  $Cal + Dol$  often surround richterite (Fig. 4c) and only scarcely enclose forsterite (Fig. 4d). In sample BLC 4, Fe-rich forsterite was almost completely replaced by Fe-rich serpentine (Fig. 4d); serpentinization is not as strong in the Fe-poor forsterite in samples BLC 1 and BLC 2. **Richterite** forms equidimensional to long prismatic subhedral grains locally associated with subhedral equidimensional Fe-rich forsterite. The textural relationships of the two minerals do not indicate any apparent replacement features (Fig. 4b). Accessory minerals include interstitial sulfides (Tab. 2), which are very common in thin sections BLC 1 and BLC 2. Phlogopite, molybdenite, oxide minerals and barite occur solely in the thin section BLC 4 (Tab. 2).

**The Na-rich actinolite + diopside assemblage** (samples BLC 3, BLC 6) exhibits relatively large grain size

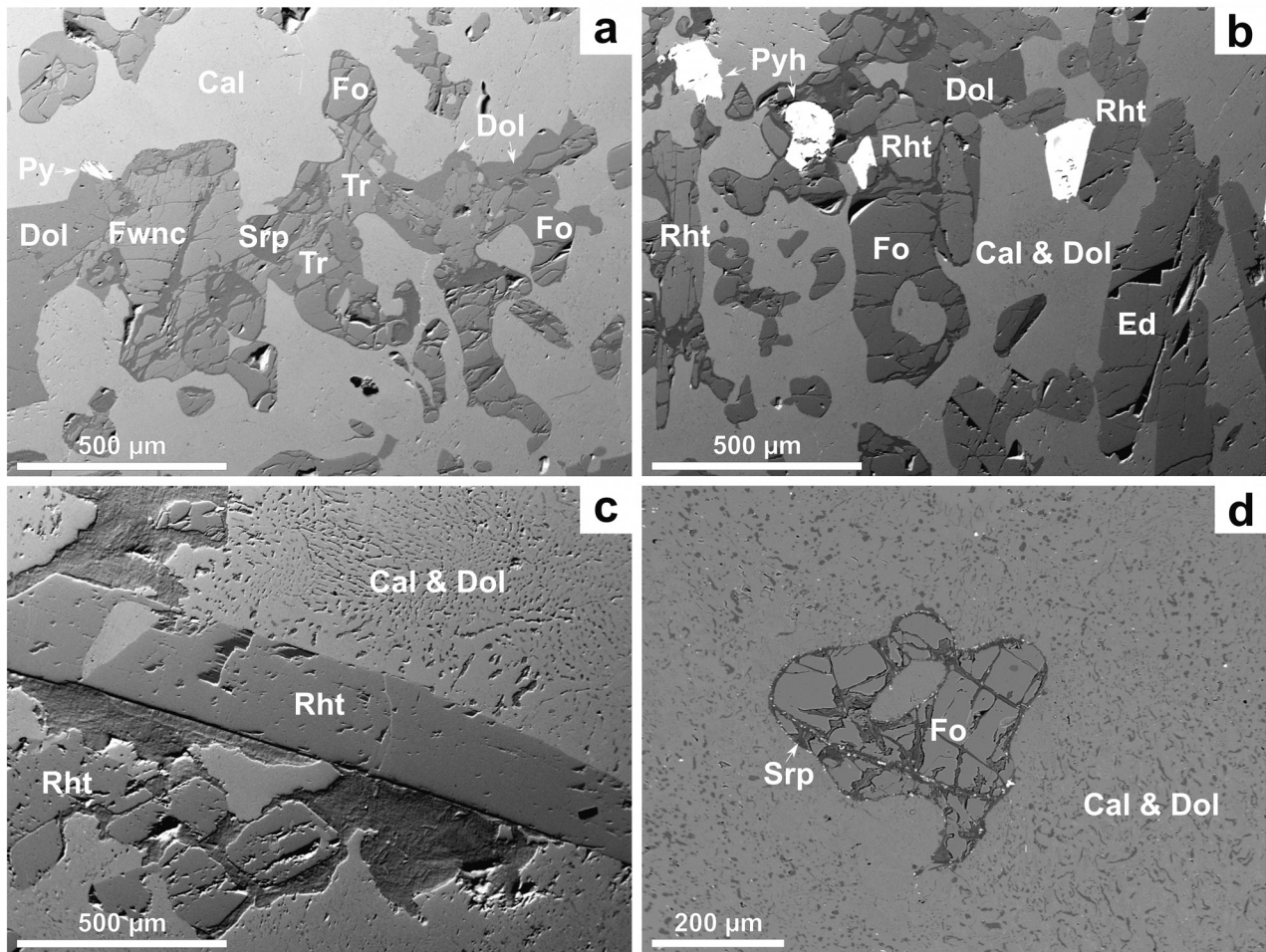


**Fig. 4** BSE images of richterite-forsterite assemblage. **a** –, **b** – are taken from the BLC 2 sample. **c** –, **d** – from BLC 4 sample. Note the alteration of forsterite and amphibole by the serpentine and textural equilibrium of forsterite and amphiboles.

**Tab. 2** Assemblages of accessory minerals.

assemblage & sample	RF			AD		HD	
	BLC 1	BLC 2	BLC 4	BLC 3	BLC 6	BLC 5	BLC 7
betafite				x			
ilmenite				x			
magnetite				x	x		
columbite				x			
pyrite	x	x	x	x		x	
pyrrhotite	x	x	x	x	x	x	
molybdenite	x	x	x	x	x	x	x
galenite	x	x	x		x		x
chalcopyrite	x	x			x		
native Bi							x
apatite				x	x	x	x
monazite				x			
xenotime							x
thorite					x	x	x
zircon						x	
barite					x	x	x
celsian							x

Magnesio-hastingsite is scarcely replaced by ferri-winchite, actinolite (Fig. 6b) and locally also by serpentine. Subhedral to anhedral grains of albite are often adjacent to (Fig. 6d) or replaced by prismatic grains of magnesio-hastingsite. Albite is also enclosed in calcite; it locally contains inclusions of zircon (Fig. 6e). Ba,Fe-rich phlogopite is typically enclosed in magnesio-hastingsite (Fig. 6a) and locally replaced by chlorite. Euhedral flakes of molybdenite, up to 7 mm in size, along with accessory fluorapatite, uranothorite (Fig. 6f) and sulfides, are common (Tab. 2).

(~2–5 mm), complex textural relations and two distinct mineral associations distributed rather randomly within the thin sections. The association  $Di + Act + Rht + Cal > Phl$  is dominant, whereas the association  $Act + Cal$  is less common. Small euhedral to subhedral grains of **richterite** are often enclosed in large subhedral grains of pale green diopside, up to 4 mm in size, and both minerals are in textural equilibrium (Fig. 5a). However, local replacement of diopside by anhedral to subhedral richterite to Na-rich actinolite was also observed (Fig. 5b,c). Subhedral grains of **Na-rich actinolite** that occur separated from diopside in the association  $Act + Cal$  have diffuse zoning with Fe-enriched, Na-depleted rims, and they are locally replaced by **ferri-winchite** (Fig. 5d). Long prismatic grains of Na-rich actinolite are locally overgrown by bluish-black **magnesio-riebeckite** with strong pleochroism ( $X =$  bluish,  $Y =$  blue,  $Z =$  deep blue) also forms quite a large individual bluish-black acicular crystals and fibrous aggregates. Locally, magnesio-riebeckite is associated with talc (Fig. 5e). Diopside locally exhibits an irregular patchy Na,Fe-zoning near its replacement by amphibole (Fig. 5c). Phlogopite is locally replaced by chlorite. The rich assemblage of accessory minerals includes sulfides, fluorapatite, betafite-pyrochlore, and uranothorite (Tab. 2, Fig. 5f).

**The magnesio-hastingsite + diopside assemblage** (samples BLC 5, BLC 7) is coarse-grained (~3–6 mm) and the primary mineral assemblage  $Mhst + Di + Cal > Ab + Phl$  is rather variable, diopside may locally prevail over magnesio-hastingsite; both minerals exhibit moderate pleochroism in green colors. **Magnesio-hastingsite** forms elongated subhedral to euhedral grains (Fig. 6a,b,d) and contains small inclusions of Ba,Fe-rich phlogopite and molybdenite (Fig. 6a).

## 4.2. Chemical composition of amphiboles, pyroxene and associated minerals

### 4.2.1. Amphiboles

The heterogeneity of the rock is also reflected in the composition of amphiboles. Different amphibole species are found in separate layers and within the individual assemblages and as single grains. They differ primarily in  $Mg/(Mg + Fe_{tot})$  ratio and concentrations of F,  $Fe^{3+}$  and Na. Representative amphibole analyses are provided in Tab. 3. To report results, we use the most recent IMA amphibole supergroup classification and nomenclature (Hawthorne et al. 2012; Fig. 7a–d); in the discussion, we compare the results with the earlier classification (Leake et al. 1997) that uses Si content instead of  $Fe_{calc}^{3+} + Al + 2Ti$  (Fig. 7e–g).

**The richterite + forsterite assemblage** is characterized by the dominance of Na–Ca amphiboles represented by richterite and very rare ferri-winchite (Fig. 7, 8; Tab. 3). They are enriched in  $F = 0.612–0.792$  apfu and the  $Mg/(Mg + Fe_{tot})$  ratio is high (0.927–1.000). They are relatively poor in Al ( $\leq 0.389$  apfu) and Ti ( $\leq 0.039$  apfu). Quite rare tremolite and edenite were identified as the only Ca-amphiboles. However, their composition with elevated  $(Na + K)_{tot} = 0.881–1.211$  apfu and  $F = 0.535–0.709$  apfu is very close to that of Na–Ca amphiboles.

Sodium-calcium amphiboles are also present in the Na-rich actinolite + diopside assemblage. Richterite to ferri-katophorite commonly replace diopside and are compositionally very similar to the richterite from the RF-assemblage; they differ by slightly higher  $^c(Al + Fe^{3+})$  and lower  $Mg/(Mg + Fe_{tot})$  ratio of 0.818–0.914 only (Tab. 3). This association is typically characterized by clusters of Na-rich actinolite (Ca-amphibole) with diffuse

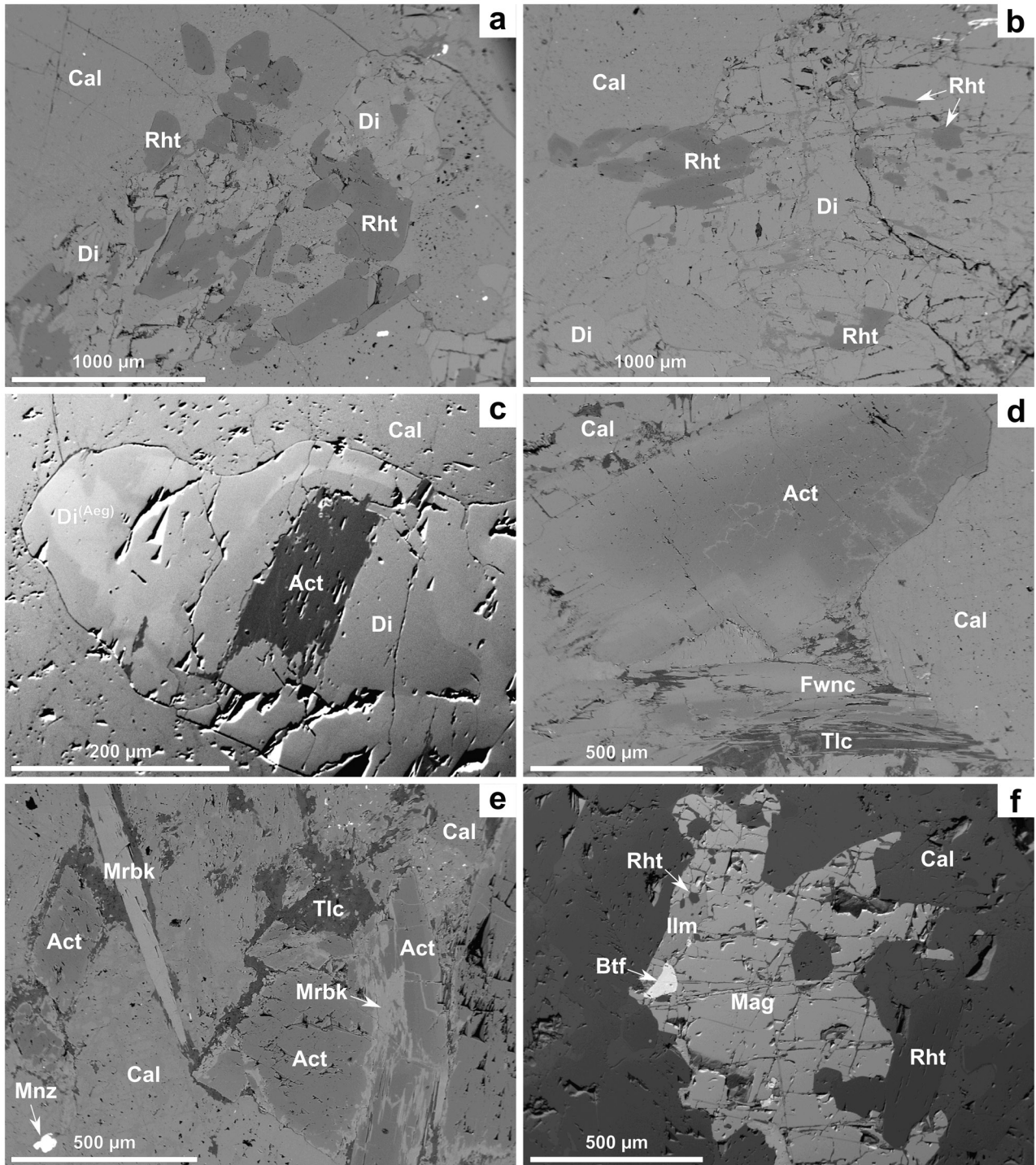


**Fig. 5** BSE images of actinolite-diopside assemblage; **a** –, **e** –, **f** – are from the BLC 3 sample, **b** –, **c** –, **d** – from the BLC 6 sample; note replacement of zoned diopside by actinolite in (**c**), zoned amphibole in (**d**), and magnesio-riebeckite rims around actinolite in (**e**).

zoning that grades to ferri-winchite (Na–Ca-amphibole) at crystal rims. The content of F is variable (0.194–0.686 *apfu*), but generally lower than in richterite. Commonly, actinolite and ferri-winchite have very contrasting rims consisting of magnesio-riebeckite, which belongs to Na-amphiboles. It is the only member of this subgroup in

the studied samples. Compared to the other amphiboles, magnesio-riebeckite has a dramatically higher content of  $^{23}\text{Na}$  reaching up to 1.873 *apfu*, and significantly high  $\text{Fe}_{\text{tot}} = 2.580\text{--}2.932$  *apfu*. The ratio of  $\text{Fe}^{3+}/(\text{Fe}^{3+} + \text{Fe}^{2+})_{\text{calc}}$  ranges between 0.606 and 0.731. Fluorine concentrations are typically low  $\leq 0.180$  *apfu*.

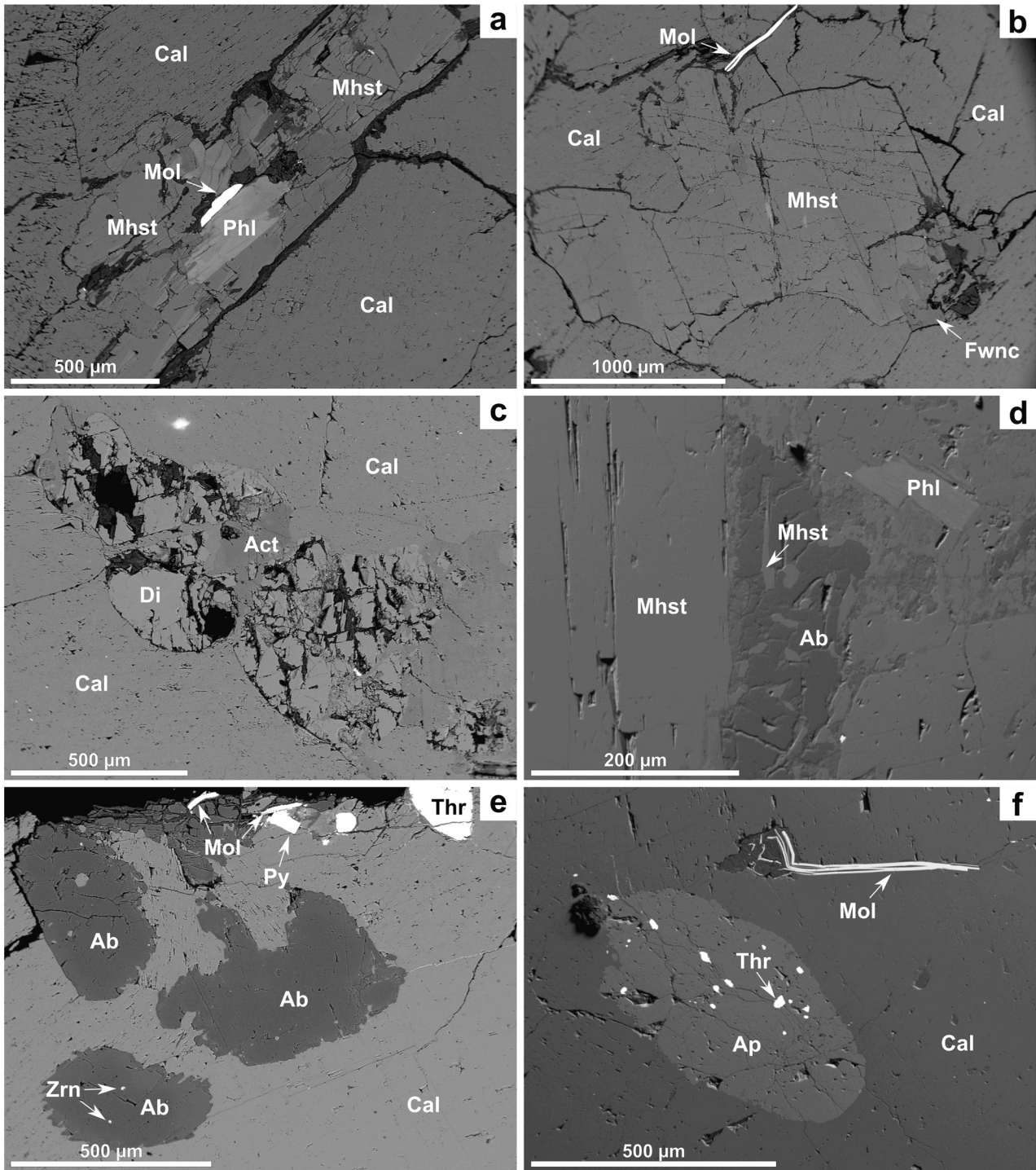


Fig. 6 BSE images of hastingsite-diopside assemblage. a – b –, c –, e –, f – are from BLC 7 sample, d – from BLC 5.

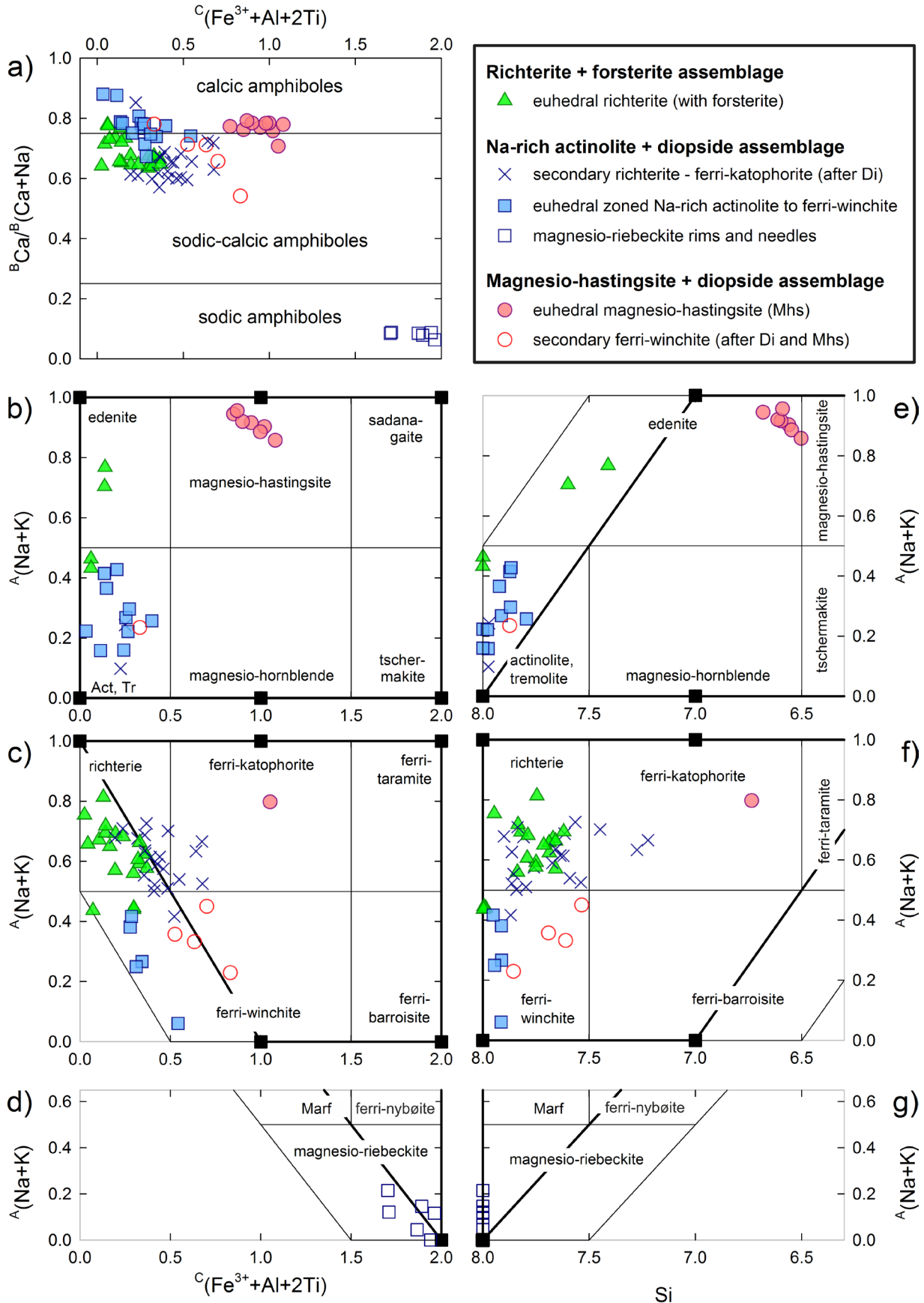
**Magnesio-hastingsite + diopside assemblage** is dominated by Ca-amphibole magnesio-hastingsite. The *T*-position is substantially occupied by <sup>7</sup>Al, reaching 1.309–1.497 *apfu*. The Mg/(Mg + Fe<sub>tot</sub>) ratio and F contents are relatively low, reaching 0.658–0.694 and 0.385–0.514 *apfu*, respectively. Diopside and

rarely magnesio-hastingsite are occasionally replaced by ferri-winchite (Na–Ca-amphibole) and actinolite (Ca-amphibole). Apart from <sup>7</sup>Al (< 0.465 *apfu*), subtly lower Fe<sub>tot</sub> (0.996–1.640 *apfu*) and F (0.205–0.411 *apfu*), they are almost isochemical with magnesio-hastingsite.

Tab. 3 Representative chemical analyses of amphiboles.

species sample/ analysis	primary												secondary				
	Rht	Rht	Tr	Rht	Rht	Fktp	Act	Fwnc	Act	Mhst	Mhst	Mhst	Mrbk	Mrbk	Fwnc	Fwnc	
	BLC4/ 86-16	BLC2/ 128-16	BLC2/ 119-16	BLC6/ 35-21	BLC3/ 45-21	BLC6/ 98-16	BLC6/ 23-21	BLC6/ 27-21	BLC3/ 50-21	BLC7/ 69-21	BLC7/ 74-21	BLC7/ 83-21	BLC3/ 47-21	BLC3/ 52-21	BLC5/ 25-16	BLC7/ 79-21	
P <sub>2</sub> O <sub>5</sub> (wt. %)	0.01	0.03	0.00	–	–	0.00	–	–	–	–	–	–	–	–	0.01	–	
SiO <sub>2</sub>	55.94	54.84	57.83	53.55	55.45	50.55	56.24	56.63	56.84	45.39	44.80	45.25	55.42	55.81	53.83	55.07	
TiO <sub>2</sub>	0.27	0.16	0.00	0.28	0.47	0.37	0.16	0.20	0.09	0.79	0.24	0.27	0.09	0.10	0.17	0.10	
Al <sub>2</sub> O <sub>3</sub>	1.16	2.38	0.02	2.34	1.63	4.49	0.87	0.94	0.03	8.56	9.49	8.88	0.25	0.31	2.70	2.02	
V <sub>2</sub> O <sub>3</sub>	0.04	0.00	0.00	–	–	0.01	–	–	–	–	–	–	–	–	0.03	–	
Cr <sub>2</sub> O <sub>3</sub>	0.00	0.00	0.00	0.00	0.00	0.00	0.00	0.00	0.01	0.00	0.00	0.01	0.02	0.00	0.00	0.01	
MnO	0.24	0.12	0.10	0.32	0.21	0.28	0.34	0.31	0.30	0.52	0.44	0.40	0.04	0.05	0.32	0.27	
Fe <sub>2</sub> O <sub>3</sub> *	2.67	0.89	0.56	3.33	3.75	5.72	0.81	2.24	2.47	4.58	7.23	6.32	15.08	17.49	5.00	5.70	
FeO*	0.17	0.00	0.00	2.66	1.70	2.37	5.54	4.41	6.55	7.93	6.21	7.04	8.92	5.78	5.77	8.61	
FeO <sub>tot</sub>	2.57	0.80	0.50	5.66	5.07	7.52	6.27	6.42	8.77	12.06	12.71	12.73	22.49	21.53	10.26	13.75	
MgO	22.43	23.47	23.64	20.34	21.18	19.00	20.07	19.77	18.82	14.53	14.65	14.77	10.11	10.37	17.29	14.65	
NiO	0.01	0.02	0.00	0.12	0.00	0.01	0.00	0.01	0.01	0.00	0.07	0.03	0.00	0.10	0.04	0.00	
ZnO	0.02	0.00	0.03	0.11	0.31	0.00	0.03	0.08	0.01	0.08	0.01	0.00	0.06	0.18	0.16	0.05	
CaO	8.58	9.68	10.46	8.84	8.82	9.38	10.52	9.88	10.20	9.65	10.02	9.99	1.09	0.81	9.39	7.07	
SrO	–	–	–	0.03	0.03	–	0.00	0.00	0.00	0.00	0.00	0.00	0.00	0.03	–	0.03	
BaO	–	–	–	0.02	0.01	–	0.00	0.00	0.00	0.04	0.11	0.09	0.00	0.00	–	0.00	
Na <sub>2</sub> O	4.41	4.32	3.16	4.54	4.37	3.91	3.00	2.80	2.52	4.52	4.71	4.22	7.25	7.10	3.12	4.12	
K <sub>2</sub> O	0.76	0.51	0.19	0.79	0.62	0.81	0.13	0.18	0.02	0.69	0.87	0.83	0.09	0.09	0.30	0.05	
F	1.71	1.61	1.24	1.47	1.56	1.30	0.91	0.94	0.78	0.92	0.95	0.89	0.28	0.29	0.61	0.45	
Cl	0.01	0.03	0.02	0.00	0.00	0.00	0.01	0.02	0.02	0.02	0.02	0.01	0.02	0.00	0.02	0.01	
H <sub>2</sub> O*	1.34	1.49	1.63	1.43	1.43	1.48	1.71	1.70	1.76	1.60	1.61	1.63	1.94	1.96	1.83	1.88	
Total	99.75	99.53	98.87	100.16	101.52	99.67	100.34	100.09	100.41	99.81	101.44	100.65	100.67	100.48	100.57	100.09	
T-site																	
P ( <i>apfu</i> )	0.001	0.004	0.000	–	–	0.000	–	–	–	–	–	–	–	–	0.001	–	
Si	7.790	7.619	8.000	7.565	7.673	7.223	7.873	7.911	7.979	6.682	6.510	6.612	8.000	8.000	7.611	7.856	
Al	0.190	0.377	0.000	0.389	0.266	0.756	0.127	0.089	0.006	1.318	1.490	1.388	0.000	0.000	0.388	0.144	
Fe <sup>3+</sup>	0.019	0.000	0.000	0.046	0.060	0.021	0.000	0.000	0.015	0.000	0.000	0.000	0.000	0.000	0.000	0.000	
C-site																	
Ti	0.028	0.017	0.000	0.030	0.049	0.040	0.017	0.021	0.010	0.087	0.027	0.030	0.010	0.011	0.018	0.011	
Al	0.000	0.013	0.003	0.000	0.000	0.000	0.016	0.066	0.000	0.167	0.135	0.142	0.043	0.053	0.061	0.196	
V	0.004	0.000	0.000	–	–	0.001	–	–	–	–	–	–	–	–	0.004	–	
Cr	0.000	0.000	0.000	0.000	0.000	0.000	0.000	0.000	0.001	0.000	0.000	0.001	0.002	0.000	0.000	0.001	
Fe <sup>3+</sup>	0.260	0.093	0.058	0.308	0.330	0.594	0.085	0.236	0.245	0.508	0.791	0.695	1.638	1.887	0.532	0.612	
Fe <sup>2+</sup>	0.020	0.000	0.000	0.315	0.196	0.283	0.649	0.515	0.769	0.976	0.754	0.861	1.077	0.693	0.682	1.028	
Mn <sup>2+</sup>	0.031	0.016	0.014	0.063	0.055	0.034	0.045	0.046	0.037	0.073	0.063	0.053	0.012	0.037	0.060	0.038	
Mg	4.657	4.861	4.876	4.284	4.370	4.048	4.188	4.117	3.939	3.188	3.173	3.218	2.175	2.217	3.644	3.115	
B-site																	
Ca	1.280	1.441	1.551	1.337	1.307	1.436	1.577	1.479	1.534	1.522	1.561	1.564	0.169	0.124	1.423	1.081	
Sr	–	–	–	0.003	0.002	–	0.000	0.000	0.000	0.000	0.000	0.000	0.000	0.002	–	0.002	
Ba	–	–	–	0.001	0.001	–	0.000	0.000	0.000	0.002	0.006	0.005	0.000	0.000	–	0.000	
Na	0.720	0.559	0.449	0.659	0.690	0.564	0.423	0.521	0.466	0.475	0.433	0.431	1.831	1.873	0.577	0.917	
A-site																	
Na	0.471	0.604	0.398	0.584	0.481	0.518	0.392	0.236	0.218	0.815	0.895	0.766	0.198	0.100	0.278	0.221	
K	0.135	0.090	0.034	0.143	0.109	0.147	0.023	0.031	0.003	0.130	0.162	0.154	0.017	0.016	0.054	0.008	
W-site																	
F	0.758	0.713	0.549	0.656	0.684	0.586	0.404	0.420	0.350	0.433	0.441	0.415	0.133	0.130	0.277	0.208	
OH	1.242	1.384	1.505	1.344	1.316	1.414	1.596	1.580	1.650	1.567	1.559	1.585	1.867	1.870	1.723	1.792	
assemblage	RF	RF	RF	AD	HD	HD	HD	AD	AD	HD	HD						

Calculations are based on the sum of cations in sites T+C = 13 *apfu*, or Si = 8 *apfu*; fields marked with a dash were not analyzed; \* – calculated from stoichiometry.



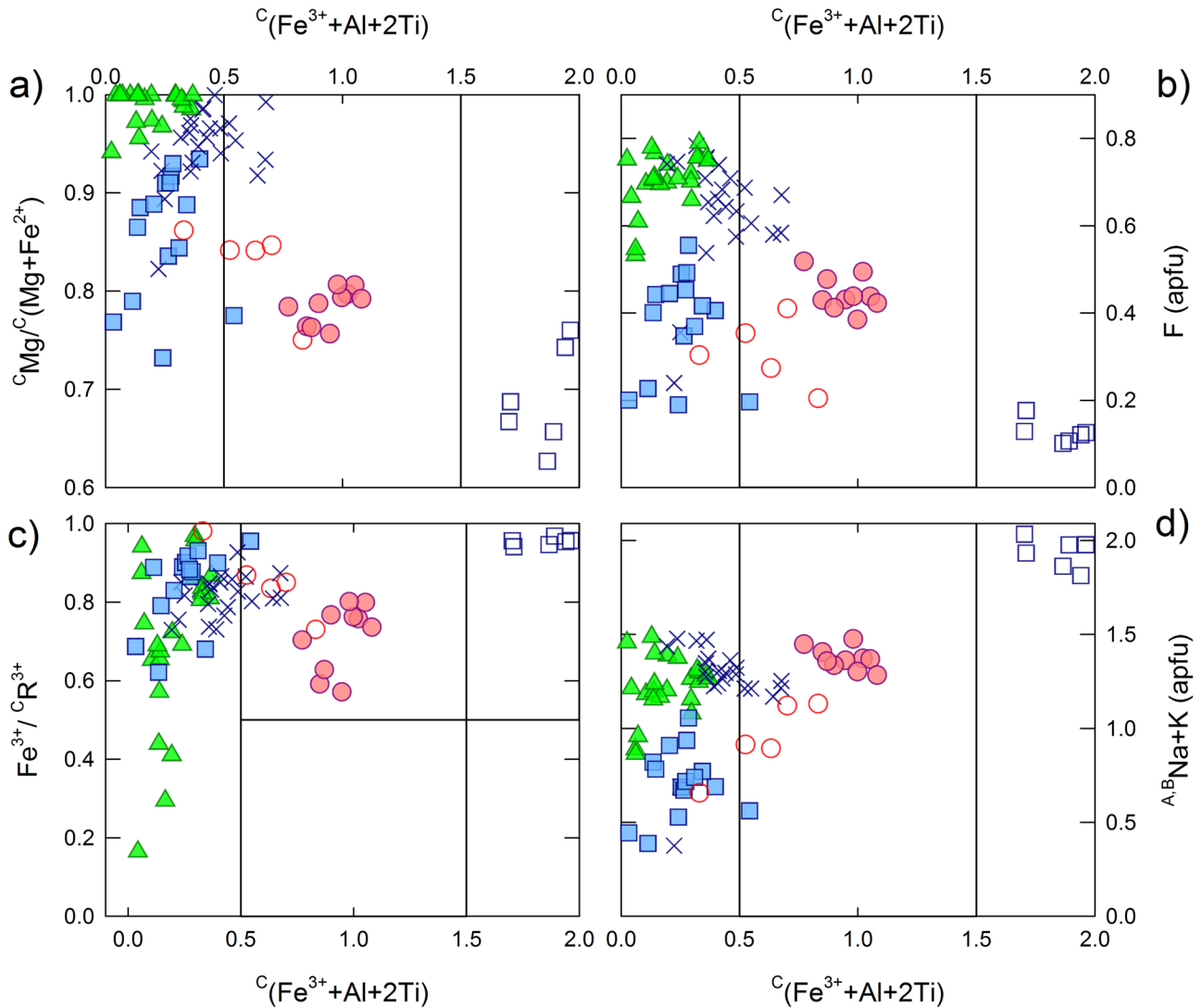


Fig. 8 Compositional variability of amphiboles. Symbols are the same as in Fig. 7.

#### 4.2.2. Pyroxene and other associated minerals

The minerals associated with amphiboles – pyroxene, olivine, phlogopite and albite – also show large compositional variations and unusual compositions (Tab. 4; Fig. 9). Diopside evolves from Na, Fe-poor (0.80 wt. %  $\text{FeO}_{\text{tot}}$ , 0.024 *apfu* Fe) in the RF-assemblage to Na, Fe-

enriched (8.55–5.37 wt. %  $\text{FeO}_{\text{tot}}$ ; 0.268–0.168 *apfu* Fe) in the AD-assemblage and Na, Fe-rich (9.53–11.07  $\text{FeO}_{\text{tot}}$ ; 0.294–0.343 *apfu* Fe) in the HD-assemblage. A positive correlation of  $\text{Fe}^{3+}$  with Na indicates the general diopside–aegirine solid solution, with the aegirine component in diopside reaching up to 17 mol. %. Within the individual assemblages, the diopside component is rather stable (Fig. 9a) and the major substitution can be the best expressed by the  $(\text{NaFe}^{3+})(\text{CaFe}^{2+})_{-1}$  vector that represents hedenbergite–aegirine substitution.

Calcite in all three assemblages (Tab. 5) shows a variable degree of enrichment in MgO (up to 3.49, 0.47, 0.71 wt. %), SrO (up to 0.39, 0.55 and 0.33 wt. %), MnO (up to 0.55, 0.92, and 0.52 wt. %), BaO (up to 0.33, 0.17, and 0.21 wt. %) and FeO (up to 0.59, 0.58, and 0.67 wt. % in RF, AD, and HD assemblages, respectively). Dolomite present in the RF-assemblage also shows elevated SrO ( $\leq 0.14$  wt. %) and MnO ( $\leq 0.57$  wt. %) contents.

⇐

Fig. 7 Classification diagrams for the individual amphibole assemblages (a–d after Hawthorne et al. 2012, and e–g after Leake et al. 1997). a – classification diagram discerning calcium, sodium–calcium, and sodium amphiboles. b –, e – classification diagrams for calcium amphiboles. c –, f – classification diagrams for sodium–calcium amphiboles. d –, g – classification diagrams for sodium amphiboles. The heavy solid black line is a two-dimensional section of amphibole composition space, the thick solid lines show the possible range of amphibole compositions in the respective subgroup (for details, see Hawthorne et al. 2012). Marf = magnesio-arfvedsonite.

**Tab. 4** Representative chemical analyses of pyroxene, forsterite, phlogopite and albite.

sample/ analysis	pyroxene							forsterite		phlogopite				albite
	BLC1/ 14-16	BLC6/ 110-16	BLC6/ 30-21	BLC3/ 44-21	BLC5/ 63-16	BLC7/ 67-16	BLC7/ 92-21	BLC1/ 20-16	BLC4/ 15-21	BLC4/ 1-21	BLC4/ 2-21	BLC7/ 67-21	BLC7/ 81-21	BLC5/ 29-16
P <sub>2</sub> O <sub>5</sub> (wt. %)	0.01	0.02	–	–	0.04	0.00	–	0.03	–	–	–	–	–	0.00
SiO <sub>2</sub>	55.88	53.84	54.10	53.99	53.37	53.73	52.57	42.81	39.56	42.40	42.09	37.34	37.44	67.36
TiO <sub>2</sub>	0.04	0.01	0.03	0.08	0.15	0.01	0.03	0.02	0.00	0.55	0.57	2.59	1.21	–
Al <sub>2</sub> O <sub>3</sub>	0.66	0.08	0.00	0.31	1.90	1.16	1.67	0.00	0.00	11.52	11.12	13.52	13.12	19.37
V <sub>2</sub> O <sub>3</sub>	0.01	0.03	–	–	0.00	0.00	–	0.00	–	0.00	0.01	0.03	0.00	–
Cr <sub>2</sub> O <sub>3</sub>	0.00	0.00	0.02	0.01	0.00	0.00	0.00	0.00	0.00	–	–	–	–	–
Fe <sub>2</sub> O <sub>3</sub> *	0.78	2.93	5.95	6.41	7.42	4.83	8.86							0.50
FeO*	0.09	3.42	0.90	2.11	3.63	5.19	2.04							
FeO <sub>tot</sub>	0.80	6.06	6.25	7.88	10.30	9.54	10.02	3.01	13.53	3.78	3.82	14.28	12.50	0.45
MgO	17.93	14.86	15.20	13.74	11.30	12.01	11.65	55.02	44.83	25.79	25.04	16.16	17.61	–
CaO	24.93	22.22	22.42	22.19	19.33	19.74	20.36	0.03	0.03	0.02	0.09	0.05	0.00	0.27
MnO	0.19	0.43	0.51	0.33	0.33	0.48	0.49	0.57	0.95	0.03	0.03	0.14	0.06	–
NiO	0.00	0.03	0.00	0.05	0.00	0.00	0.00	0.01	0.00	0.00	0.02	0.03	0.00	–
ZnO	0.10	0.03	0.06	0.07	0.00	0.11	0.00	0.00	0.26	0.02	0.04	0.00	0.03	–
SrO	–	–	0.03	0.00	–	–	0.02	–	0.00	0.00	0.00	0.00	0.00	–
BaO	–	–	–	–	–	–	–	–	0.00	0.98	0.93	3.01	5.66	0.35
Na <sub>2</sub> O	0.56	1.19	1.60	1.98	3.26	2.53	2.91	0.02	0.00	0.75	0.46	0.40	0.73	11.49
K <sub>2</sub> O	0.00	0.02	0.00	0.00	0.02	0.01	0.00	0.00	0.01	9.11	9.22	7.93	6.43	0.06
F	–	–	–	–	–	–	–	0.11	0.00	2.78	1.42	0.76	1.08	–
Cl	–	–	–	–	–	–	–	0.01	0.02	0.01	0.03	0.03	0.06	–
H <sub>2</sub> O*										2.83	3.40	3.28	3.24	
Total	101.19	99.11	100.81	101.27	100.75	99.79	100.60	101.65	99.19	100.56	98.26	99.54	99.17	99.35
P ( <i>apfu</i> )	0.000	0.001	–	–	0.001	0.000	–	0.001	0.000	–	–	–	–	0.000
Si	1.993	1.999	1.974	1.973	1.967	1.998	1.944	1.004	0.999	3.021	3.049	2.845	2.875	2.978
Ti	0.001	0.000	0.001	0.002	0.004	0.000	0.001	0.000	0.000	0.030	0.031	0.148	0.070	–
Al	0.028	0.004	0.000	0.013	0.083	0.051	0.073	0.000	0.000	0.967	0.949	1.214	1.187	1.009
V	0.000	0.001	–	–	0.000	0.000	–	0.000	0.000	0.000	0.000	0.000	0.000	–
Cr	0.000	0.000	0.001	0.000	0.000	0.000	0.000	0.000	0.000	0.000	0.000	0.002	0.000	–
Fe <sup>3+</sup>	0.021	0.082	0.163	0.176	0.206	0.135	0.247							0.037
Fe <sup>2+</sup>	0.003	0.106	0.027	0.064	0.112	0.161	0.063	0.059	0.286	0.225	0.232	0.910	0.803	
Mg	0.953	0.822	0.827	0.748	0.621	0.666	0.642	1.923	1.688	2.739	2.704	1.835	2.016	–
Ca	0.953	0.884	0.876	0.869	0.763	0.787	0.807	0.001	0.001	0.002	0.007	0.004	0.000	0.013
Mn	0.006	0.013	0.016	0.010	0.010	0.015	0.015	0.011	0.020	0.002	0.002	0.009	0.004	–
Ni	0.000	0.001	0.000	0.001	0.000	0.000	0.000	0.000	0.000	0.000	0.001	0.002	0.000	–
Zn	0.003	0.001	0.002	0.002	0.000	0.003	0.000	0.000	0.005	0.001	0.002	0.000	0.002	–
Sr	–	–	0.001	0.000	–	–	0.000	0.000	0.000	0.000	0.000	0.000	0.000	–
Ba	–	–	–	–	–	–	–	0.000	0.000	0.027	0.026	0.090	0.170	0.006
Na	0.039	0.086	0.113	0.140	0.233	0.183	0.208	0.001	0.000	0.103	0.064	0.058	0.109	0.985
K	0.000	0.001	0.000	0.000	0.001	0.000	0.000	0.000	0.000	0.828	0.852	0.771	0.630	0.003
F	–	–	–	–	–	–	–	0.008	0.000	0.627	0.325	0.184	0.263	–
Cl	–	–	–	–	–	–	–	0.000	0.001	0.001	0.003	0.003	0.008	–
OH										1.343	1.641	1.665	1.659	
assemblage	RF	AD	AD	AD	HD	HD	HD	RF	RF	RF	RF	HD	HD	HD

Formulae calculations of pyroxene and forsterite are based on sum of all cations (4 and 3 *apfu*, respectively), formulae of micas are based on 12 anions. Albite formula is based on 4 anions. Fields marked with a dash were not analyzed; \* – calculated from stoichiometry.

Forsterite from the thin sections BLC 1 and BLC 2 is Fe-poor (2.87–3.01 wt. % FeO<sub>tot</sub>; 0.058–0.062 *apfu* Fe<sup>2+</sup>) whereas BLC 4 is Fe-enriched (13.34–13.53 wt. %; 0.286–0.282 *apfu* Fe<sup>2+</sup>). Phlogopite evolves from

F-rich (0.627–0.325 *apfu*) and Fe-poor (0.225–0.232 *apfu*) phlogopite in BLC 4 (RF) to Ba, Fe, Ti-enriched phlogopite in BLC 7 (HD; Fig. 9b). Albite from the HD-assemblage is Ca-poor (0.05–0.40 wt. % CaO) and

K-poor (0.04–0.11 wt. %  $K_2O$ ) but enriched in Ba ( $\leq 0.69$  wt. % BaO) and Fe ( $\leq 0.50$  wt. %  $Fe_2O_{3tot}$ ).

## 5. Discussion

### 5.1. Nomenclature of amphiboles

Amphiboles found in the individual assemblages were classified using the scheme by Hawthorne et al. (2012) based on the sum of octahedrally-coordinated trivalent cations and Ti – (Al +  $Fe^{3+}$  + 2Ti). This classification differs from the earlier one in some cases based on the Si content (Leake et al. 1997). Both schemes are shown in Fig. 7; the main differences include:

- 1) amphibole classified as magnesio-hastingsite falls to the  $Fe^{3+}$ -rich edenite field in Leake's (1997) classification due to its relatively high Si ( $> 6.5$  apfu).
- 2) analyses plotting near the ferri-katophorite–richterite border of the Hawthorne et al. (2012) classification, in some cases fall within the richterite field ( $Fe^{3+}$ -rich richterite), rarely in ferri-katophorite field.

The examined amphibole assemblages show the advantage of simultaneous use of both schemes for petrological studies as the differences help distinguish anomalous compositions. Classification of the amphiboles found in Bližná is slightly complicated because their contents of Na at the B-site typically fall near the 0.5 apfu  $^{23}Na$  boundary (Fig. 7a) that divides calcic amphiboles from sodic–calcic amphiboles (Hawthorne et al. 2012). In some cases, it is necessary to use additional adjectives and indicate

the transitional composition (e.g., Na-rich actinolite to ferri-winchite) as the bare mineral name would lack the petrological information.

### 5.2. Substitutions and compositional variations in amphiboles and associated minerals

In general, the composition of amphiboles evolves from tremolite to richterite or from tremolite to magnesio-rie-

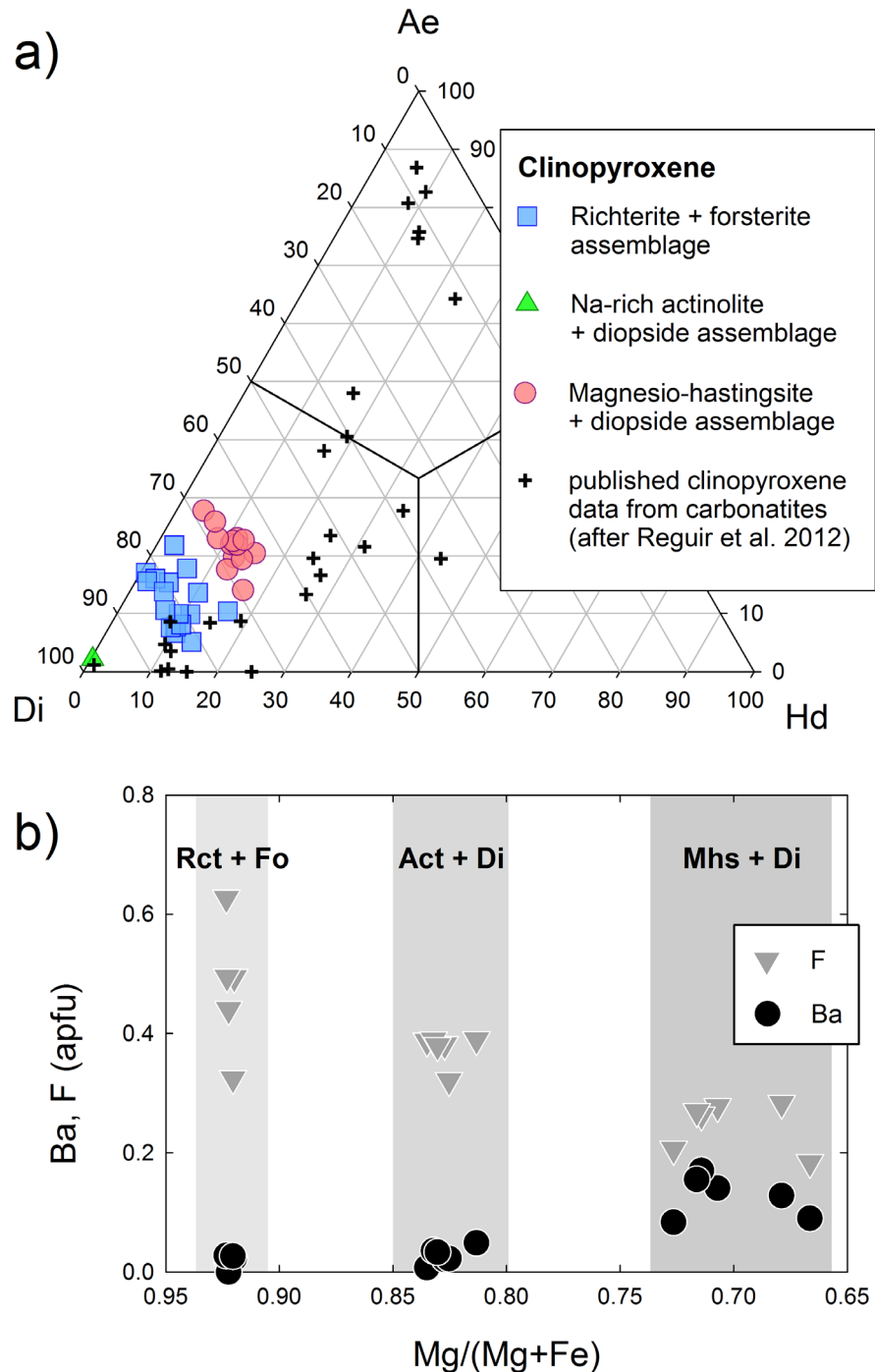


Fig. 9 Composition of pyroxene and phlogopite; a – clinopyroxene in the Bližná assemblages, compared to the published data (after Reguir et al. 2012); b – composition of phlogopite in the Bližná assemblages.

**Tab. 5** Representative chemical analyses of carbonates.

sample/ analysis	calcite				dolomite	
	BLC2/ 122-16	BLC4/ 33-21	BLC3/ 55-21	BLC7/ 78-21	BLC4/ 88-16	BLC2/ 130-16
MgO (wt. %)	3.49	1.43	0.47	0.64	18.97	19.51
CaO	51.66	52.48	54.11	54.17	30.65	31.22
MnO	0.27	0.50	0.92	0.52	0.57	0.28
FeO	0.15	0.58	0.58	0.67	1.91	0.37
SrO	0.12	0.35	0.00	0.33	0.14	0.06
BaO	0.00	0.33	0.17	0.04	0.00	0.00
CO <sub>2</sub>	44.66	44.18	43.60	44.10	46.35	46.23
Total	100.34	99.85	99.85	100.46	98.58	97.67
Mg ( <i>apfu</i> )	0.085	0.036	0.012	0.016	0.894	0.922
Ca	0.908	0.943	0.966	0.964	1.038	1.060
Mn	0.004	0.007	0.013	0.007	0.015	0.007
Fe <sup>2+</sup>	0.002	0.008	0.008	0.009	0.051	0.010
Sr	0.001	0.003	0.000	0.003	0.003	0.001
Ba	0.000	0.000	0.000	0.000	0.000	0.000
C	1.000	1.000	1.000	1.000	2.000	2.000
assemblage	RF	RF	AD	HD	RF	RF

Formula calculations are based on cation sums (1 *apfu* for calcite, 2 *apfu* for dolomite).

beckite (Fig. 7a, 8d); this is characterized by the exchange of Na for Ca via substitution (<sup>A</sup>Na<sup>B</sup>Na)<sub>1</sub>(<sup>A</sup>□<sup>B</sup>Ca)<sub>-1</sub> or increase of Na<sub>tot</sub> along with Fe<sup>3+</sup> content, respectively (Fig. 8d). The two exchanges are accompanied by homovalent substitutions such as Fe<sup>2+</sup>Mg<sub>-1</sub>, F<sub>1</sub>(OH)<sub>-1</sub> and to a lesser extent, also Fe<sup>3+</sup>Al<sub>-1</sub> (Fig. 8a–c). The increase of richterite component is accompanied by the increase of Mg/(Mg + Fe<sup>2+</sup>) and F contents, whereas the increase of trivalent cations at the octahedral site is followed by their decrease (Fig. 8a–c). Most amphiboles are fairly heterogeneous to estimate compositional trends of individual generations; however, the amphiboles in the magnesio-hastingsite + diopside assemblage follow the substitution (<sup>A</sup>Na<sup>C</sup>R<sup>2+</sup>)<sub>1</sub>(<sup>A</sup>□<sup>C</sup>R<sup>3+</sup>)<sub>-1</sub> along with Tschermak's substitution (<sup>C</sup>R<sup>3+</sup>TAl<sup>3+</sup>)<sub>1</sub>(<sup>C</sup>R<sup>2+</sup>TSi)<sub>-1</sub>; both are documented by the variable <sup>A</sup>Na, <sup>C</sup>(Fe<sup>3+</sup> + Al + 2Ti), Fe<sup>3+</sup>/(Fe<sup>3+</sup> + Al) and Si contents (Figs. 7b, c, e, f and 8d).

There is a general increase in Fe contents in amphiboles in the RF via the AD to the HD-assemblage, with an obvious overlap of the latter two assemblages (Fig. 8a–d). Late magnesio-riebeckite from the AD-assemblage (BLC 3) shows <sup>A</sup>Na-, and Fe<sup>3+</sup>-enrichment towards magnesio-arfvedsonite (Fig. 7d,g). The concentrations of F generally decrease with increasing Fe, from F-rich richterite to F-poor magnesio-riebeckite (Fig. 8b). Well-defined negative correlation Fe/F indicates a potential Fe/F avoidance in the amphibole structure (e.g., Rosenberg and Foit 1977) known in other silicates (e.g., biotite – Mason 1992); however, lower availability of F in late fluids facilitating origin of magnesio-riebeckite is more likely due to the absence of F in late-stage

minerals. Concentrations of Na are variable but similar in all assemblages except for the late Na-rich magnesio-riebeckite (Fig. 8d). Magnesio-hastingsite from the HD-assemblage is enriched in Al (Fig. 8a–d).

The amphibole composition (Fig. 10a) partially overlaps with the carbonatite field defined by Reguir et al. (2012) and the amphibole composition range from the Fir carbonatite, Canada (Chudy 2013); however, the overlap is relatively poor and does not clearly indicate the relationship of the Bližná carbonatite-like marble to carbonatites.

Diopside compositions evolve from Al-poor diopside in the RF-assemblage to the diopside with up to 17 mol. % of aegirine component in the HD-assemblage (Tab. 4, Fig. 9a). They generally fall into the carbonatite field defined by Reguir et al. (2012). However, pyroxenes of similar composition are not uncommon in alkaline igneous rocks (e.g., Martin 2007). Calcite in all three assemblages has elevated concentrations of Mg, Sr, Mn, Ba and Fe and this enrichment is similar to carbonates from the Fir carbonatite, British Columbia, Canada (Chudy 2013). The rock-forming calcite shows elevated Sr and high Mn abundances (Tab. 5), characteristic of carbonatites, which are uncommon in sedimentary carbonates and distinctly higher from ordinary marbles in the Moldanubian Zone. The latter typically contain low levels of Sr and Mn not exceeding 100 ppm (e.g., Veizer et al. 1992). Yang and Le Bas (2004) suggested that the Sr and Mn contents of carbonate minerals can be used to discriminate igneous rocks from metamorphosed sedimentary carbonates. Ca, K-poor albite enriched in Ba and Fe from the HD-assemblage is somewhat unique in its composition; its BaO and Fe<sub>2</sub>O<sub>3</sub> contents (≤ 0.69 wt. % BaO and ≤ 0.50 wt. % Fe<sub>2</sub>O<sub>3tot</sub>) seem to be the highest reported in Ca, K-poor albite up to date. Elevated amounts of Fe<sub>2</sub>O<sub>3</sub> in plagioclase (0.24 wt. % in albite Ab<sub>100</sub> and up to 0.44 wt. % Fe<sub>2</sub>O<sub>3</sub> in Ca-rich plagioclase An<sub>77</sub>Ab<sub>20</sub>Or<sub>1</sub>) were reported from Mont Saint Hilaire alkaline pegmatites (Schilling et al. 2011), from Thor Lake alkaline pegmatite (in albite Ab<sub>98</sub>; up to 0.20 wt. % Fe = 0.28 wt. % Fe<sub>2</sub>O<sub>3tot</sub>; De St. Torre and Smith 1988), and from Bayan Obo carbonatite dykes (0.20 FeO<sub>tot</sub> = 0.22 wt. % Fe<sub>2</sub>O<sub>3tot</sub> in Ab<sub>100</sub>; Le Bas et al. 1992). The presence of Fe-enriched plagioclase seems to be significant in alkaline rocks; however, a systematic study is needed to make conclusive interpretations.

### 5.3. Comparison of amphiboles and other minerals from ordinary metacarbonates of the Moldanubian Zone (Bohemian Massif) and banded metacarbonate in Bližná

Amphiboles from the examined carbonatite-like marble in Bližná differ significantly from amphiboles in ordi-

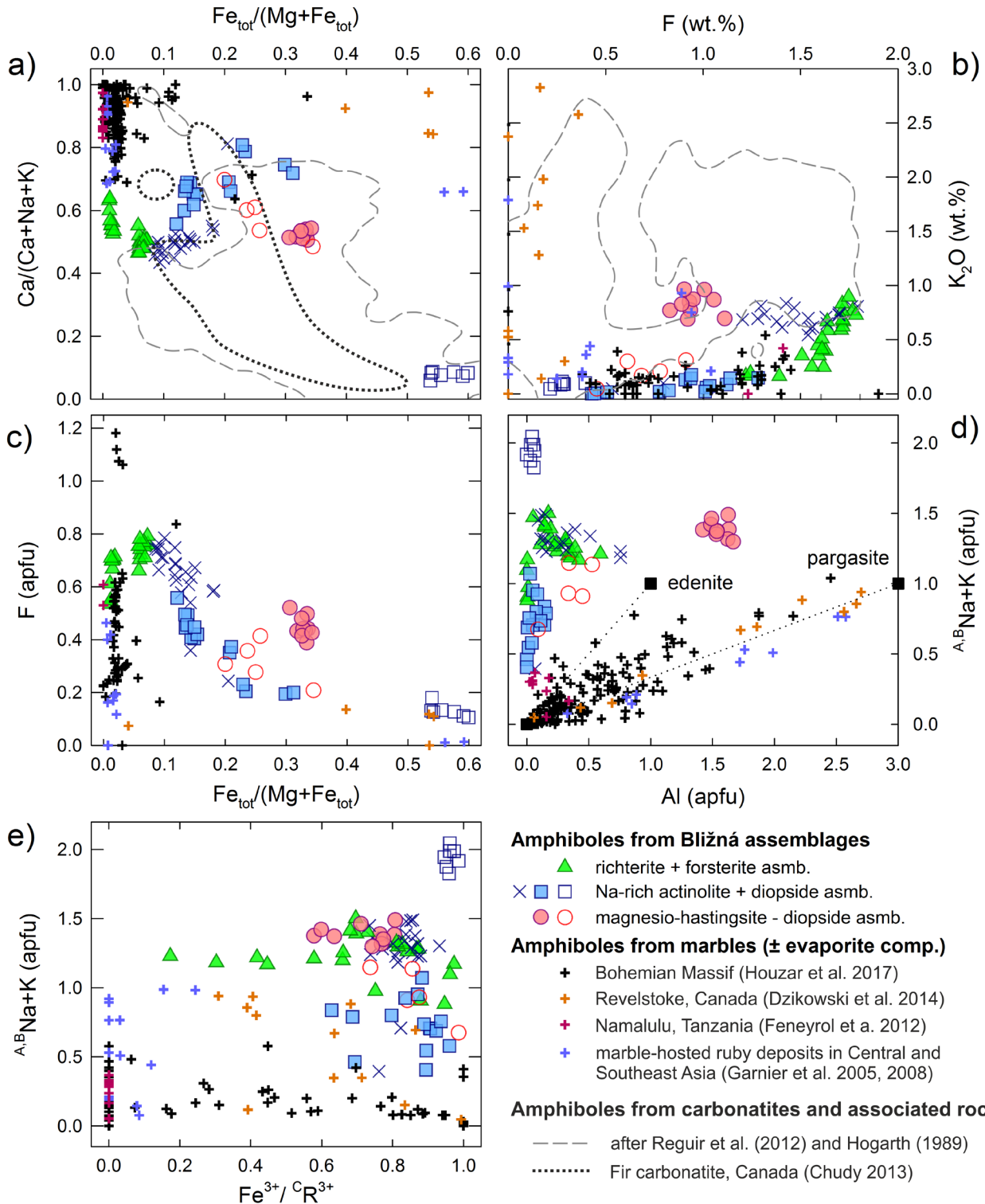


**Fig. 10** Comparison of Bližná amphiboles composition to **a**–**b** – the amphiboles from carbonatites (after Reguir et al. 2012; Hogarth 1989; Chudy 2013) and **(a–e)** to the amphiboles from ordinary marbles in the Bohemian Massif (Houzar 2004; Houzar et al. 2017) and marble hosted-ruby deposits (Garnier et al. 2005, 2008; Feneyrol et al. 2012; Dzikowski et al. 2014).

nary marbles of the Moldanubian Zone as well as other geological units (for instance Olešnice unit, Velké Vrbno unit, Vratěnin unit, Vranov unit and other localities in the

Český Krumlov unit; Novák 1989; Houzar 2004), where typically calcic amphiboles (tremolite, edenite, pargasite, magnesio-hornblende) occur (Fig. 10). The major dif-

ferences in the composition include significantly higher Na, Fe, and F contents in Bližná (Fig. 10). Only scarcely, Na-bearing fluor-tremolite ( $< 0.5 \text{ apfu Na}_{\text{tot}}$ ) associated with fluor-uvite in hydrothermal vein cutting marble was identified in Muckov; it is the only amphibole showing a slight compositional similarity to amphiboles from the carbonatite-like marble in Bližná. In the RF-assembly, chemical compositions of diopside and forsterite are comparable to ordinary dolomite marbles except for the BLC 4 sample, where forsterite is enriched in Fe. However, the composition of the associated richterite (Tab. 3) markedly differs from the usual tremolite in ordinary marbles. Similarly, diopside with high aegirine component and Ba-enriched phlogopite from AD- and HD-assembly are distinct from their counterparts described in ordinary marbles, the latter mainly by its high Fe contents (cf. Doležalová et al. 2006; Houzar and Cícha 2016; Houzar et al. 2017).

#### 5.4. Origin of the Bližná mineral assemblages

The Bližná marble shows mostly plastic deformation and dynamic recrystallization of carbonates along with brittle deformation of silicate bands. The calcite + dolomite symplectites observed in Bližná are typical for some carbonatites (e.g., Chudy 2013; Chakhmouradian et al. 2016a). They are interpreted as an exsolution texture after a high-temperature carbonate solid solution; the texture is typically magmatic (Chakhmouradian et al. 2016a). Chudy (2013) calculated the carbonate solvus temperatures and concluded that they mostly represent regional peak-metamorphic conditions, but part of the samples represented the original magmatic crystallization; the Cal+Dol exsolution texture is a result of retrograde re-equilibration of the carbonatites.

The observed amphibole parageneses and compositions do not indicate prograde overprint of the potential magmatic amphibole assemblages; similarly, Reguir et al. (2012) and Chudy (2013) interpret most amphibole compositions in carbonatites as magmatic. In Bližná, euhedral amphiboles seem to be in equilibrium with forsterite, diopside or Ba, Fe-rich phlogopite, and their formation is earlier or coeval with crystallization of oxides (Fig. 5f). In the HD assemblage, albite formed in disequilibrium with diopside resulting in reaction  $\text{Ab} + \text{Di} = \text{Mhst}$ ; excess of albite allowed the formation of the  $\text{Mhst} + \text{Ab}$  intergrowths (Fig. 6d). The secondary ferri-katophorite to richterite forming after diopside and magnesio-riebeckite overgrowths around Na-rich actinolite and ferri-winchite require input of Na, F and minor Fe and Na and  $\text{Fe}^{3+}$  under oxidizing conditions, respectively, probably during post-magmatic evolution of the rock. On the other hand, the breakdown of  $\text{Mhst}$  to ferri-winchite might be related to retrograde hydration reactions in the marble, similar

to the formation of serpentine and talc at the expense of Mg-silicates (Fig. 6b).

Formation of late sodic amphibole (magnesio-riebeckite, magnesio-arfvedsonite or ferri-nyboite) is characteristic of carbonatites attributed to autometasomatic overprint by late-stage alkaline fluids (Hogarth 1989; Chakhmouradian and Zaitsev 2002; Reguir et al. 2012, Chudy 2013); origin from Na, Fe-rich fluids agrees with the observed replacement of actinolite by magnesio-riebeckite in the Bližná carbonatite-like marble (Fig. 5e).

#### 5.5. Origin of carbonatite-like marble

We discuss the potential origin of the carbonatite-like marble from Bližná based mainly on the chemical composition of amphiboles and associated minerals, their compositional trends, and the mineral assemblages and textural relations of minerals. Accessory minerals (Tab. 2) are considered, too, although these have not been studied in detail in this paper. An obvious metamorphic overprint hampers the evaluation of the potential origin of carbonatite-like marble. However, we examine several potential options.

(i) Metacarbonates (potentially with Na- and Na, Ca-carbonates and sulfate admixture) are a product of sedimentation in a limnic (playa) and/or hypersaline lagoonal environments with potential production of evaporites. Accessory sodic, and sodic-calcic amphiboles and sodic-ferric pyroxenes in these particular sediments may be of detritic or diagenetic origin (Milton and Eugster 1959; Fortey and Michie 1978; Mange-Rajetzky 1981; Behr et al. 1983; Decarreau et al. 2004). Metamorphic amphiboles that reflect the input of evaporite component (commonly associated with scapolite) are known from marble-hosted ruby and tsavorite deposits (e.g., Garnier et al. 2005, 2008; Feneyrol et al. 2012; Dzikowski et al. 2014). However, a total absence of Cl and/or B in the assemblage (e.g., marialite and tourmaline described from other marbles within the Český Krumlov Unit and elsewhere in the Bohemian Massif; e.g., Kadounová 1987; Kříbek 1988; Kříbek et al. 1997; Bačík et al. 2012; Krmíček et al. 2021) does not support the hypothesis for marine evaporite source. Moreover, marbles with significant evaporite component typically contain amphiboles with tremolite–pargasite or tremolite–edenite solid solution with variable  $^{\text{A,B}}(\text{Na} + \text{K}) < 1 \text{ apfu}$ , elevated Al (Fig. 10d), variable F and locally high  $\text{K}_2\text{O}$  contents (Fig. 10b), and commonly very low  $\text{Fe}_{\text{tot}}/(\text{Mg} + \text{Fe}_{\text{tot}})$  and  $\text{Fe}^{3+}/\text{R}^{3+}$  (Fig. 10c,e). These amphibole compositions are distinctly different from magnesio-riebeckite and the early amphiboles from Bližná that represent primarily actinolite–richterite solid solution (Fig. 7, 10d).

(ii) Admixture of volcanodetritic component (basic tuffs, tuffites or mixed sediments) during carbonate

sedimentation (Kadounová 1987; Hladíková et al. 1993; Drábek and Stein 2015; Drábek et al. 2017) is an additional option. Tholeitic amphibolites are relatively common in the Český Krumlov Unit; however, alkaline rocks such as metabasites which would represent a source of some components (Na, Ba, Fe, F) in the marble have not been found in the Černá region (Patočka 1991; Janoušek et al. 2008). Nevertheless, their potential presence in this region cannot be discounted. Besides the presence of Na, Fe-rich silicate assemblages, this option does not explain the presence of Nb-oxides (Drábek et al. 2017) nor the anomalous composition of carbonates.

(iii) Metamorphosed carbonatites enclosed in ordinary sedimentary metacarbonate show distinct geochemical signatures (Drábek et al. 1999; Novák et al. 2012), and are characterized by the occurrence of Na, Fe, F-enriched amphiboles, Sr, Mn-enriched carbonates (Tucker and Wright 1990; Veizer et al., 1992; Yang and Le Bas 2004; Cheng et al. 2010; Chakhmouradian et al. 2016b), and diopside with elevated aegirine component (Reguir et al. 2012). The Bližná occurrence shows a remarkable similarity with the Fir carbonatite, British Columbia (Chudy 2013), representing a suite of dolomite- and calcite-dominated carbonatites with variable contents of silicates, apatite and sulfides, and fenitized mafic country rocks, metamorphosed under amphibolite-facies conditions. Both localities feature Sr, Mn-enriched Fe, Mg-bearing calcite, amphiboles ranging from Na-rich actinolite–edenite and magnesio-hastingsite through richterite–winchite–katophorite to magnesio-riebeckite (–magnesio-arfvedsonite–nyböite), as well as the clinopyroxene–albite assemblage (retrograde, formed at the expense of magnesio-hastingsite in the Fir carbonatite).

The Bližná amphiboles are similar to those from carbonatites in their high Na and elevated Fe contents but differ in lower Al abundances. In carbonatites, assimilation of crustal material is regarded as a possible source of Al (e.g., Chakhmouradian and Zaitsev 2002); its limited presence in Bližná may therefore indicate the relatively pristine composition of the examined small part of the metacarbonate sequence.

(iv) Sodium-rich metasomatites characterized by mineral assemblages with Na, Fe, F-enriched amphiboles, diopside with high aegirine component and albite (e.g., Albino 1995; Potts 2000; Shi et al. 2003; Yiming and Daxin 2005; Tsikos and Moore 2005; Hogarth 2016) are another potential option. Drábek and Stein (2015) claim that there is no textural or other geological evidence for the input of fluids from the host rocks; the role of external fluids needs to be assessed by the petrographic study of carbonates. We observed hydrothermal overprint in thin sections (e.g., Fig. 5b–e, 6a–c), but the fluids were not particularly rich in F and their Fe content increases with the decrease of F (Fig. 10c).

## 6. Conclusions

Three distinct mineral assemblages were recognized in carbonatite-like marble from Bližná – richterite + forsterite assemblage ( $Rht + Fo + Cal > Dol > Phl + Di$ ), Na-rich actinolite + diopside assemblage ( $Di + Act + Rht + Cal > Phl$ ) and magnesio-hastingsite + diopside assemblage ( $Mhst + Di + Cal > Ab + Phl$ ). The following amphibole species were recognized in the individual assemblages: RF – (richterite > ferri-winchite > tremolite, edenite), AD – (actinolite > ferri-winchite; richterite > ferri-katophorite; magnesio-riebeckite), HD – (magnesio-hastingsite) using the scheme of Hawthorne et al. (2012).

The individual mineral assemblages differ especially in  $Mg/(Mg + Fe^{tot})$  ratio and F concentrations. Diopside contains up to 17 mol. % of the aegirine component and albite is Fe, Ba-enriched. The compositional ranges of amphibole and diopside are very similar to carbonatites *s.l.* and suggest highly alkaline conditions typical for carbonatites. The following possible origin of the carbonatite-like marble from Bližná are examined: (i) metacarbonates potentially with Na- and Na, Ca-carbonates and sulfate admixture; (ii) admixture of volcanodetritic component during carbonate sedimentation; (iii) metamorphosed carbonatites (or their dykes) enclosed in ordinary sedimentary metacarbonate; (iv) Na-rich metasomatites characterized by mineral assemblages with Na, Fe, F-enriched amphiboles, diopside with high aegirine component and albite. We can exclude (i) marine evaporates rich in Cl or B because amphibole assemblages are free of Cl and B, whereas the other options (ii), (iii) and (iv) are, in general, possible.

The amphiboles observed in the Bližná carbonatite-like marble are unique within the Bohemian Massif and distinctly different from amphiboles found in metacarbonates with evaporite component (Fig. 10a–e). A thorough study of the whole mineral assemblage, including isotopic studies, is required to reveal the original protolith of the rock and assess the metamorphic changes in the marble body.

*Acknowledgments.* The authors dedicate this article to the late Milan Drábek for his long-term and fundamental research in mineralogy, experimental petrology and economic geology, including the examined metacarbonates from Bližná. The authors are grateful for the thorough reviews of the manuscript by D. Zozulya and an anonymous reviewer and for the editorial suggestions and corrections by J. Kotková. This work was supported by the research project GAČR 19-17276S to MN, RŠ and JC. The article appears through the institutional support of long-term conceptual development of research institutions provided by the Ministry of Culture (ref. MK000094862) to SH.

## References

- ALBINO GV (1995) Sodium Fault metasomatism along Zone, Sierra Nevada California, USA the Melones Foothills. *Mineral Mag* 59: 383–399
- BAČÍK P, UHER P, CEMPÍREK J, VACULOVÍČ T (2012) Magnesian tourmalines from plagioclase-muscovite-scapolite metaevaporite layers in dolomite marble near Prosetín (Olešnice Unit, Moravicum, Czech Republic). *J Geosci* 57: 143–153
- BEHR HJ, AHRENDT H, MARTIN H, PORADA H, RÖHRS J, WEBER K (1983) Sedimentology and Mineralogy of Upper Proterozoic Playa-Lake Deposits in the Damara Orogen. In: Martin H, Eder FW (eds) *Intracontinental Fold Belts. Case Studies in the Variscan Belt of Europe and the Damara Belt in Namibia*, Springer, Berlin, Heidelberg, pp 577–610
- CHÁB J, BREITER K, FATKA O, HLADIL J, KALVODA J, ŠIMŮNEK Z, ŠTORCH P, VAŠÍČEK Z, ZAJÍC J, ZAPLETAL J (2008) Brief geology of the basement of the Bohemian Massif and its Carboniferous and Permian cover. *Czech Geological Survey, Praha*, pp 1–283 (in Czech)
- CHAKHMOURADIAN AR, ZAITSEV AN (2002) Calcite amphibole clinopyroxene rock from the Afrikanda complex, Kola Peninsula, Russia: mineralogy and a possible link to carbonatites. III. Silicate minerals. *Canad Mineral* 40: 1347–1374
- CHAKHMOURADIAN AR, REGUIR EP, ZAITSEV AN (2016a) Calcite and dolomite in intrusive carbonatites. I. Textural variations. *Mineral Petrol* 110(2-3): 333–360
- CHAKHMOURADIAN AR, REGUIR EP, COUĚSLAN C, YANG P (2016b) Calcite and dolomite in intrusive carbonatites. II. Trace-element variations. *Mineral Petrol* 110: 361–377
- CHENG X, KYNICKÝ J, CHAKHMOURADIAN AR, QI L, SONG W (2010) A unique Mo deposit associated with carbonatites in the Qinling orogenic belt, central China. *Lithos* 118: 50–60
- CHUDY TC (2013) The petrogenesis of the Fir carbonatite system, east-central British Columbia, Canada. PhD thesis, University of British Columbia, pp 1–560
- ČÍZEK J, KRÍBEK B, BOUZEK F, HLADÍKOVÁ J, ŠMEJKAL V (1984) Izotopická kompozice karbonátů z grafitových ložisek Česko-uherského Varied Unit, Moldanubicum. *Sborník "Korelace proterozoických a paleozoických stratiformních ložisek"* 8: 103–122 (in Czech)
- DECARREAU A, PETIT S, VIELLARD P, DABERT N (2004) Hydrothermal synthesis of aegirine at 200 °C. *Eur J Mineral* 16: 85–90
- DEER WA, HOWIE RA, ZUSSMAN J (1997) *Double Chain Silicates, Rock-Forming Minerals*, (2<sup>nd</sup> edition.) vol. 2B. The Geological Society, London, UK, pp 764
- DE ST. TORRE L, SMITH DGW (1988) Cathodoluminescent gallium-enriched feldspars from the Thor Lake rare-metal deposits, Northwest Territories. *Canad Mineral* 26: 301–308
- DOLEŽALOVÁ H, HOUZAR S, LOSOS Z, ŠKODA R (2006) Kinoshitalite with a high magnesium content in sulphide-rich marbles from the Rožná uranium deposit, Western Moravia, Czech Republic. *N Jb Min, Abh*, 2006 2: 165–171
- DRÁBEK M, STEIN H (2003) The age of formation of a marble in the Moldanubian Varied Group, Bohemian Massif, Czech Republic using Re-Os dating of molybdenite. In: Eliopoulos D, et al. (eds) *Mineral exploration and sustainable development – Proceed SGA meeting, Athens*, 973–976
- DRÁBEK M, STEIN H (2015) Molybdenite Re–Os dating of Mo–Th–Nb–REE rich marbles: pre-Variscian processes in Moldanubian Variegated Group (Czech Republic). *Geol Carpath* 66: 173–179
- DRÁBEK M, FRÝDA J, JANOUŠEK V (1999) Regionally metamorphosed carbonatite-like marbles from the Varied Group, Moldanubian Unit, Bohemian Massif, Czech Republic, and their Mo–Th–Nb–REE mineralization. – In: Stanley CJ (ed.): *Proceedings of the fifth biennial SGA meeting and the tenth quadrennial IAGOD meeting, London*, pp 635–638
- DRÁBEK M, FRÝDA J, ŠARBACH M, SKÁLA R (2017) Hydroxycalcio-pyrochlore from a regionally metamorphic marble at Bližná, Southwestern Czech Republic. *N Jb Mineral Abh* 194: 49–59
- DZIKOWSKI TJ, CEMPÍREK J, GROAT LA, DIPPLE GM, GIULIANI G (2014) Origin of gem corundum in calcite marble: The Revelstoke occurrence in the Canadian Cordillera of British Columbia. *Lithos* 198: 281–297
- FENEYROL J, OHNENSTETTER D, GIULIANI G, FALLICK AE, ROLLION-BARD C, ROBERT JL, MALISA EP (2012) Evidence of evaporites in the genesis of the vanadian grossular 'tsavorite' deposit in Namalulu, Tanzania. *Canad Mineral* 50: 745–769
- FORTEY NJ, MICHIE UMCL (1978) Aegirine of possible authigenic origin in Middle Devonian sediments in Caithness, Scotland. *Mineral Mag* 42: 439–442
- FRANK W, HAMMER S, POPP F, SCHARBERT S, THONI M (1990) Isotopengeologische Neuergebnisse zur Entwicklungsgeschichte der Bohmischen Masse: Proterozoische Gesteinsserien und Variszische Hauptorogenese. *Osterr Beitr Met Geoph* H3: 185–228
- FRANK W, SCHARBERT S, HÖCK V (1992) Rb/Sr - Untersuchungen an Karbonatgestein der Böhmisches Masse. FWF - Projekte S4702 und S4704. In: Höck V (ed.) *Schwerpunktprogramm S47 GEO „Präalpidische Kruste in Österreich“ Bericht 1991*, pp 9–10
- GARNIER V, OHNENSTETTER D, GIULIANI G, MALUSKI H, DELOULE E, TRONG TP, VAN LP, QUANG VH (2005) Age and significance of ruby-bearing marble from the Red River Shear Zone, northern Vietnam. *Canad Mineral* 43: 1315–1329
- GARNIER V, GIULIANI G, OHNENSTETTER D, FALLICK AE, DUBESSY J, BANKS D, VINH HQ, LHOMME T, MALUSKI

- H, PECHER A, BAKHSH KA, VAN LONG P, TRINH PT, SCHWARZ D (2008) Marble-hosted ruby deposits from Central and Southeast Asia: Towards a new genetic model. *Ore Geol Rev* 34: 169–191
- HAWTHORNE FC, OBERTI R, HARLOW GE, MARESCH WV, MARTIN RF, SCHUMACHER JC, WELCH MD (2012) Nomenclature of the amphibole supergroup. *Amer Mineral* 97: 2031–2048
- HLADÍKOVÁ J, KŘÍBEK B, MACENAUER T (1993) Isotopic composition of sulphidic sulphur in the graphitic deposits of the Bohemian Massif. *Věst Čes Geol ústavu* 68: 65–71
- HOGARTH DD (1989) Pyrochlore, apatite and amphibole: distinctive minerals in carbonatite. – In: Bell, K. (Ed.), *Carbonatites: Genesis and Evolution*. Unwin Hyman, London, pp 105–148
- HOGARTH DD (2016) Chemical Trends in the Meech Lake, Québec, Carbonatites and Fenites. *Canad Mineral* 54 (5): 1105–1128
- HÖGELSBERGER H (1989) Die Marmore und Kalksilikatgesteine der Bunten Serie – Petrologische Untersuchungen und geologische Konsequenzen. *Jb Geol B-A* 132: 213–230
- HOUZAR S, CÍCHA J (2016) Chondrodite- and clinohumite-bearing marbles of the Podolsko Complex in Písek area and related F-rich Mg–Si–Ti–Ba–Zr mineral assemblage (Moldanubian Zone, Bohemian Massif). *Bull mineral-petrolog Odd Nár Muz (Praha)* 24: 33–45 (in Czech)
- HOUZAR S (2004) Metamorphosed carbonate rocks in geology and evolution at the south-eastern margin of the Bohemian Massif. Unpublished PhD thesis Masaryk University Brno, pp 3–155 (in Czech)
- HOUZAR S, NOVÁK M (2002) Marbles with carbonatite-like geochemical signature from variegated units of the Bohemian Massif, Czech Republic, and their geological significance. *J Czech Geol Soc* 47 (3–4): 103–109
- HOUZAR S, NOVÁK M, CÍCHA J (2017) Mineral assemblages and lithology of marbles of the Bohemian part of the Moldanubian Zone (Bohemian Massif). *Bull Mineral Petrol* 25 (2): 113–140 (in Czech)
- JANOŠEK V, VRÁNA S, ERBAN V, VOKURKA K, DRÁBEK M (2008) Metabasic rocks in the Varied Group of the Moldanubian Zone, southern Bohemia – their petrology, geochemical character and possible petrogenesis. *J Geosci* 53: 31–64
- JENČEK V, VAJNER V (1968) Stratigraphy and relations of the groups in the Bohemian part of the Moldanubicum. *Krystalinikum* 6: 105–124
- KADOUNOVÁ Z (1987) Petrology, petrochemistry and structural evolution of the Městský vrch graphite deposits and its relation to rocks of Český Krumlov Varied Group, Moldanubicum. Unpublished Diploma thesis Charles University, pp 1–134 (in Czech)
- KRMÍČEK L, NOVÁK M, TRUMBULL RB, CEMPÍREK J, HOUZAR S (2021) Boron isotopic variations in tourmaline from metacarbonates and associated calc-silicate rocks from the Bohemian Massif: Constraints on boron recycling in the Variscan orogen. *Geosci. Frontiers* 12: 219–230
- KŘÍBEK B (1988) Lithological, structural and metamorphic development of the graphite deposits in the Český Krumlov varied Group, Moldanubicum. *Sborník „Hornická Příbram ve vědě a technice“*, geologie, pp 255–270 (in Czech)
- KŘÍBEK B, HLADÍKOVÁ J, FRÝDA J (1997) Scapolite and anhydrite-bearing rocks from the Moldanubian zone of the Bohemian Massif: Metamorphosed exhalites and evaporites. *J Czech Geol Soc* 42 (3): 62
- LE BAS MJ, KELLERE J, KEJIE T, WALL F, WILLIAM CT, PEISHAN Z (1992) Carbonatite dykes at Bayan Obo, Inner Mongolia, China. *Mineral Petrol* 46: 195–228
- LEAKE B E, WOOLLEY AR, ARPS CE, BIRCH WD, GILBERT MC, GRICE JD, HAWTHORNE FC, KATO A, KISCH HJ, KRIVOVICHEV VG, LINTHOUT K, LAIRD J, MANDARINO JA, MARESCH WV, NICKEL EH, ROCK NMS, SCHUMACHER JC, SMITH DC, STEPHENSON NCN, UNGARETTI L, WHITTAKER EJW, YOUZHI G (1997) Nomenclature of amphiboles; report of the Subcommittee on Amphiboles of the International Mineralogical Association Commission on new minerals and mineral names. *Mineral Mag* 61 (405): 295–310
- MARTIN RF (2007) Amphiboles in the igneous environment. *Rev Mineral Geochem* 67: 323–358
- MANGE-RAJETZKY MA (1981) Detrital blue sodic amphibole in Recent sediments, southern coast, Turkey. *J Geol Soc* 138: 83–92
- MASON RA (1992) Models of order and iron-fluorine avoidance in biotite. *Canad Mineral* 30 (2): 343–354
- MERLET C (1994) An Accurate Computer Correction Program for Quantitative Electron Probe Microanalysis. *Mikrochim Acta* 114/115: 363–376
- MILTON C, EUGSTER HP (1959) Mineral assemblages of Green River formation. In: Abelson HP (e) *Researches in Geochemistry*; John Wiley & Sons: New York, NY, USA, pp 118–150
- MITCHELL RH (2005) Carbonatites and carbonatites and carbonatites. *Canad Mineral* 43 (6): 2049–2068
- NOVÁK M (1989) Metamorphism of dolomite rocks at the north-eastern margin of the moldanubicum, Western Moravia, Czechoslovakia. *Acta Mus Morav* 74: 7–51 (in Czech)
- NOVÁK M, ŠKODA R, GADAS P, KRMÍČEK L, ČERNÝ P (2012) Contrasting origins of the mixed (NYF+LCT) signature in granitic pegmatites, with examples from the Moldanubian zone, Czech Republic. *Canad Mineral* 50: 1077–1094
- PATOČKA F (1991) Geochemistry and Primary Tectonic Environment of the Amphibolites from the Český Krumlov Varied Group (Bohemian Massif, Moldanubicum). *Jb Geol B – A* 134: 117–133

- POTTS DA (2000) Sodium metasomatism and magnesio-riebeckite mineralization in the Wilson Ridge pluton. UNLV Retrospective Theses & Dissertations 1155: 1–117
- RADKOVÁ P (2017) Mineralogy and petrography of metacarbonate rocks from Bližná near Černá v Pošumaví. Unpublished Ms Thesis, Masaryk University, pp 1–61 (in Slovak)
- REGUIR EP, CHAKHMOURADIAN AR, PISIAK L, HALDEN NM, YANG P, XU C, KYNICKÝ J, COUĚSLAN CG (2012) Trace-element composition and zoning in clinopyroxene – and amphibole-group minerals: Implications for element partitioning and evolution of carbonatites. *Lithos* 128–131: 27–45
- ROSENBERG PE, FOIT FF (1977) Fe<sup>2+</sup>-F avoidance in silicates. *Geochim Cosmochim Acta* 41: 345–346
- ŠARBACH M, DRÁBEK M, VESELOVSKÝ F (1985) Mo–Th–Nb–lanthanoide mineralization of marble at Václav mine, Bližná. *Geol průzkum* 27: 116 (in Czech)
- SCHILLING J, MARKS MA, WENZEL T, VENNEMANN T, HORVÁTH L, TARASSOFF P, JACOB DE, MARKL G (2011) The magmatic to hydrothermal evolution of the intrusive Mont Saint-Hilaire complex: insights into the late-stage evolution of peralkaline rocks. *J Petrol* 52(11): 2147–2185
- SCHRAUDER M, BERAN A, HOERNES S, RICHTER W (1993) Constraints on the Origin and the Genesis of Graphite-Bearing Rocks From the Variegated Sequence of the Bohemian Massif (Austria). *Mineral Petrol* 49: 175–199
- SHI GH, CUI WY, TROPPER P, CHANG-QIU WANG, GUI-MING SHU, HAIXA YU (2003) The petrology of a complex sodic and sodic–calcic amphibole association and its implications for the metasomatic processes in the jadeitite area in northwestern Myanmar, formerly Burma. *Contrib Mineral Petrol* 145: 355–376
- SUK M (1974) Lithology of Moldanubian metamorphics. *Čas Mineral Geol* 19: 373–389
- TSIKOS H, MOORE JM (2005) Sodic metasomatism in the Palaeoproterozoic Hotazel iron-formation, Transvaal Supergroup, South Africa: implications for fluid–rock interaction in the Kalahari manganese field. *Geofluids* 5: 264–271
- TUCKER ME, WRIGHT VP (1990) *Carbonate Sedimentology*. Blackwell Publishing, Oxford, pp 1–482
- VEIZER J, PLUMB KA, CLAYTON RN, HINTON RW, GROTZINGER JP (1992) Geochemistry of Precambrian carbonates: V. late Paleoproterozoic seawater. *Geochim Cosmoch Acta* 56 (6): 2487–2501
- VESELOVSKÝ F, DRÁBEK M, DRÁBKOVÁ E, ŠARBACH M (1987) Marbles of carbonatite character from the Moldanubic Varied group at Bližná, Czechoslovakia. *Proceedings 1<sup>st</sup> seminar on carbonatites and alkaline rocks of the Bohemian Massif and ambient regions, Praha*, pp 85–91
- VRÁNA S, BRÍZOVÁ E, DVOŘÁK I, GRUNDLOCH J, HOLÁSEK O, KADLECOVÁ R, KREJČÍ Z, KRUPÍČKA J, LYSENKO V, MANOVÁ M, NÝVLT D, POŇAVIČ M, PŘECHOVÁ E, ŠRÁMEK J, TRUBAČ J, VERNER K (2010) Explanation to geological map of the Czech Republic 1 : 25 000, Sheet 32-233 Černá v Pošumaví. Unpublished manuscript, Czech Geological Survey, Prague, pp 1–125 (in Czech)
- WARR LN (2021) IMA–CNMNC approved mineral symbols. *Mineral Mag* 85 (3): 291–320
- YANG XM, LE BAS MJ (2004) Chemical compositions of carbonate minerals from Bayan Obo, Inner Mongolia, China: implications for petrogenesis. *Lithos* 72 (1–2): 97–116
- YIMING Z, GE B, DAXIN L (2005) REE-Nb (Fe, U, Th)-bearing alkaline skarns of China. In: Mao J., Bierlein FP (eds) *Mineral Deposit Research: Meeting the Global Challenge*. Springer, Berlin, Heidelberg, pp 507–509
- ZOUBEK V, FIALA J, VAŇKOVÁ V, MACHART J, STETTNER G (1988) Moldanubian Region. In: ZOUBEK V (ed) *Precambrian in Younger Fold Belts*, John Wiley & Sons, pp 183–267